NIH Public Access
Author Manuscript
Pain. Author manuscript; available in PMC 2013 May 01.

Published in final edited form as:
Pain. 2012 May ; 153(5): 1091–1106. doi:10.1016/j.pain.2012.02.015.

Intrathecal cannabilactone CB_2R agonist, AM1710, controls pathological pain and restores basal cytokine levels

Jenny L. Wilkerson[1,*], **Katherine R. Gentry**[2], **Ellen C. Dengler**[1], **James A. Wallace**[1], **Audra A. Kerwin**[1], **Leisha M. Armijo**[1], **Megan N. Kuhn**[3], **Ganesh A. Thakur**[4], **Alexandros Makriyannis**[4], and **Erin D. Milligan**[1,*]

[1]Department of Neurosciences, Health Sciences Center, School of Medicine, University of New Mexico, Albuquerque, NM 87131

[2]Department of Anesthesiology and Critical Care Medicine, Health Sciences Center, School of Medicine, University of New Mexico, Albuquerque, NM 87131

[3]Health Sciences Center, School of Medicine, University of New Mexico, Albuquerque, NM 87131

[4]Center for Drug Discovery, Northeastern University, Boston, MA 02115

Abstract

Spinal glial and proinflammatory cytokine actions are strongly implicated in pathological pain. Spinal administration of the anti-inflammatory cytokine, interleukin-10 (IL-10) abolishes pathological pain and suppresses proinflammatory interleukin-1β (IL-1β) and tumor necrosis factor alpha (TNF-α). Drugs that bind the cannabinoid type 2 receptor (CB_2R) expressed on spinal glia reduce mechanical hypersensitivity. To better understand the CB_2R-related anti-inflammatory profile of key anatomical nociceptive regions, we assessed mechanical hypersensitivity and protein profiles following intrathecal application of the cannabilactone CB_2R agonist, AM1710, in two animal models; unilateral sciatic nerve chronic constriction injury(CCI), and spinal application of HIV-1 glycoprotein 120 (gp120), a model of peri-spinal immune activation. In CCI animals, lumbar dorsal spinal cord and corresponding dorsal root ganglia (DRG) were evaluated by immunohistochemistry for expression of IL-10, IL-1β, phosphorylated p38-mitogen-activated-kinase (p-p38MAPK), a pathway associated with proinflammatory cytokine production, glial cell markers, and degradative endocannabinoid enzymes including monoacyl glycerol lipase (MAGL). AM1710 reversed bilateral mechanical hypersensitivity. CCI revealed decreased IL-10 expression in dorsal spinal cord and DRG while AM1710 resulted in increased IL-10, comparable to controls. Adjacent DRG and spinal sections revealed increased IL-1β, p-p38MAPK, glial markers and/or MAGL expression, while AM1710 suppressed all but spinal p-p38MAPK and microglial activation. In spinal gp120 animals, AM1710 prevented bilateral mechanical hypersensitivity. For comparison to immunohistochemistry, IL-1β and TNF-α protein quantification from lumbar spinal and DRG homogenates was determined, and revealed increased DRG IL-1β protein levels

© 2012 International Association for the Study of Pain. Published by Elsevier B.V. All rights reserved.

[*]Corresponding Authors: Jenny L. Wilkerson, University of New Mexico, HSC, Dept. of Neurosciences, MSC08-4740, 1 University of New Mexico, Albuquerque, NM 87131, JLWilkerson@salud.unm.edu, Phone: +1(505)272-4441, Fax: +1(505)272-8082. Erin D. Milligan, University of New Mexico, HSC, Dept. of Neurosciences, MSC08-4740, 1 University of New Mexico, Albuquerque, NM 87131, Emilligan@salud.unm.edu, Phone: +1(505)272-8103, Fax: +1(505)272-8082.

The authors would like to disclose a conflict of interest. A.M. is a consultant for MAK Scientific.

Publisher's Disclaimer: This is a PDF file of an unedited manuscript that has been accepted for publication. As a service to our customers we are providing this early version of the manuscript. The manuscript will undergo copyediting, typesetting, and review of the resulting proof before it is published in its final citable form. Please note that during the production process errors may be discovered which could affect the content, and all legal disclaimers that apply to the journal pertain.

NIH-PA Author Manuscript
NIH-PA Author Manuscript
NIH-PA Author Manuscript

NIH-PA Author Manuscript

NIH-PA Author Manuscript

NIH-PA Author Manuscript

from gp120, that was robustly prevented by AM1710 pretreatment. Cannabilactone CB_2R agonists are emerging as anti-inflammatory agents with pain therapeutic implications.

Keywords

cannabinoid; CCI; paraffin immunohistochemistry; rat; spectral analysis; gp120

1. Introduction

Spinal sensitization of pain projection neurons is a critical process underlying pathological pain. Unilateral chronic constriction injury (CCI) of the sciatic nerve as well as spinal inflammation following i.t. HIV-1 glycoprotein-120 (gp120) are utilized here as animal models of pathological pain. While distinctly different in etiology, both models are characterized to involve activated spinal glia and proinflammatory cytokine activity [95]. Astrocytes and microglia produce interleukin-1β (IL-1β) and tumor necrosis factor-alpha (TNF-α) which mediate pathological pain in a variety of animal models [14,76]. Glia in spinal cord dorsal horn and dorsal root ganglia (DRG)[6,33]show increases in phosphorylated p38 mitogen-activated kinase (p-p38MAPK), a MAPK strongly associated with IL-1β and TNF-α expression [28]. DRG are home to glial satellite cells that generate IL-1β and TNF-α, additionally contributing to pathological pain in response to peripheral injury[23,26,63,79,80,86,87]. Conversely, interleukin-10 (IL-10) is a critical pleiotropic anti-inflammatory cytokine that suppresses IL-1β and TNF-α actions and blocks phosphorylation of factors that activate MAPK pathways resulting in the inhibition of MAPK actions [22]. Lumbosacral intrathecal (i.t.) administration of the IL-10 transgene or protein leads to robust suppression of light touch hypersensitivity (allodynia) produced by CCI as well as spinal inflammation following i.t. gp120 [55–57].

Two cannabinoid receptor subtypes, CB_1R and CB_2R, are characterized to produce analgesic effects [85]. CB_1R are present on neurons throughout the CNS and their activation within the brain corresponds to a variety of effects beyond pain control [21]. However, CB_2R are primarily expressed on microglia [70]and peripheral immune cells including macrophages [74]. Activation of CB_2Rs lack the known central nervous system (CNS) side effects produced by CB_1R activation [8,21,70,102]. Following peripheral nerve injury, increased expression of CB_2Rs, endocannabinoids, and related degradative enzymes occur in DRG and spinal cord [41,58,94]. Reports demonstrate that the effects of CB_2R activation reduces pathological pain with a corresponding decrease in activation markers for spinal cord astrocytes, microglia, and factors associated with proinflammatory pathways [69,72,89,94]. Given the newly characterized cannabilactone, AM1710, binds CB_2R with greater affinity than CB_1R (54-fold $CB_2R>CB_1R$) [34,61], and its antinociceptive action is selectively blocked by CB_2R antagonists [68], i.t. administration of AM1710 was examined here for its potential actions to reverse or prevent allodynia produced by CCI and i.t. gp120, respectively. While prior reports reveal that spinal CB_2R activation controls pathological pain responses in neuropathic rats [66,67,69,71,102], the underlying spinal immunoregulatory signals in parallel with endocannabinoid degradative enzymes remain unclear.

The aim of the present study was to determine alterations in IL-10 immunoreactivty with concurrent reduction in immunoreactivity of CNS glial activation markers, IL-1β, p-p38MAPK, and the widely characterized endocannabinoid degradative enzymes, monoacyl glycerol lipase (MAGL) and fatty acid amine hydrolase (FAAH) in the dorsal horn and DRG in behaviorally-verified CCI neuropathic rats following i.t. application of AM1710 [34,68]. Bilateral allodynia was examined, as prior reports have documented this change

NIH-PA Author Manuscript

NIH-PA Author Manuscript

NIH-PA Author Manuscript

from normal sensory responses [55,64,65]. Following i.t. gp120, cytokine protein levels surrounding the injection site and DRG were quantified by enzyme-linked immunosorbent assay (ELISA) procedures.

2. Methods

2.1. Animals

A total of 76 pathogen-free adult male Sprague Dawley rats (300–400 gram; Harlan Labs, Madison, WI) were used in all experiments. Rats were double-housed in a temperature and light-controlled (12 hour light/dark; lights on at 6:00 AM) environment, with standard rodent chow and water available *ad libitum*. All procedures adhered to the guidelines of the Committee for Research and Ethical Issues of the International Association for the Study of Pain and were approved by the Institutional Animal Care and Use Committee (IACUC) of the University of New Mexico Health Sciences Center.

2.2. Drugs

The CB_2R agonist, 3-1(1′,1′-Dimethylheptyl)-1-hydroxy-9-methoxy-6*H*-benzo[c]-chromene-6-one (AM1710) [34,61]was used in these experiments. AM1710 was generously gifted by A.M. and G.T. AM1710 was first dissolved in 100% ethanol and diluted in sterile water (Hospira Inc, Lake Forest, IL) for a final of concentration 1 mg/ mL containing 5% ethanol. The vehicle of AM1710 was sterile water containing 5% ethanol. Pilot studies determined the dose range of AM1710, with a 100-fold dose range tested (10 μg – .1 μg in 10 μl or equivolume vehicle). Immediately prior to intrathecal (i.t.) injections, frozen (−80°C) recombinant gp120 (product 1021-2; lot number 7A3I20; ImmunoDiagnostics, Bedford, MA) was thawed, and diluted to 0.5 μg/μl with 0.1% rat serum albumen in sterile PBS, pH 7.4 (Life Technologies, Gaithersburg, MD. Three (3) μg in 6 μl or equivolume vehicle was prepared on ice as detailed in prior reports [24,52,54,82].

2.3. Behavioral assessment of allodynia

Baseline (BL) responses to light mechanical touch were assessed using the von Frey test after animals were habituated to the testing environment, as previously described [9,52]. Briefly, rats were placed a top 2 mm-thick parallel bars, spaced 8 mm apart and habituated for approximately 45 minutes for 5 days. All behavioral testing was performed during the first half of the light cycle in a sound, light, and temperature controlled room. The von Frey test utilizes a series of calibrated monofilaments, (3.61 – 5.18 log stimulus intensity; North Coast Medical, Morgan Hills, CA) applied randomly to the left and right plantar surface of the hindpaw for 8 seconds. Lifting, licking or shaking the paw was considered a response. For all behavioral testing, threshold assessment was performed in a blinded fashion by J.L.W.

2.4. Chronic constriction injury (CCI) surgery

Following BL behavioral assessment, the surgical procedure for chronic constriction of the sciatic nerve was completed as previously described[4]. Briefly, inisoflurane-(induction 5% vol. followed by 2.5% in oxygen) anesthetized rats, the mid-to lower back and the dorsal left thigh shaved and cleaned with diluted Bacti-Stat AE, (EcoLab HealthCare Division, Mississauga, Ontario, Canada). Using aseptic procedures, the sciatic nerve was carefully isolated, and loosely ligated with 4 segments of chromic gut sutures (Ethicon, Somerville, NJ). Sham surgery was identical to CCI surgery but without the nerve ligation. The overlying muscle was sutured closed with (2) 3-0 sterile silk sutures (Ethicon, Somerville, NJ), and animals recovered from anesthesia within approximately 5 minutes. Animal placement into either CCI or sham surgical groups was randomly assigned.

NIH-PA Author Manuscript

NIH-PA Author Manuscript

NIH-PA Author Manuscript

2.5. Chronic indwelling catheter surgery used for i.t. gp120 administration

Following BL assessment for light mechanical touch, chronic indwelling i.t. catheterization was performed as previously described in experiments utilizing gp120 for the induction of allodynia[50,52,54]. All animals recovered from this procedure within 5 minutes without overt signs of motor weakness or discomfort. Verification of lumbar PE-10 catheter placement was conducted at the time of tissue collection. One hundred percent of catheters were successfully placed within the intrathecal L5 lumbar region.

2.6. Intrathecal injection for chronic indwelling catheters

For chronic indwelling catheters in gp120 experiments, all drugs were pre-filled into an 'i.t. injection catheter' as detailed previously[50]. A 3-minute i.t. injection was administered in alert, conscious rats with light towel restraint. No overt motor weakness was observed. Six microliters of gp120 followed by an 8 μl sterile saline flush during a 10 second interval was injected.

2.7 Acute intrathecal injection used in CCI-related experiments

In rats with CCI, all drugs were administered via acute i.t. catheter placement. Injections were performed as previously described[52]. Either 10 μl drug or equivolume vehicle was withdrawn into the injection catheter, which was gently inserted and threaded rostrally to the 7.7 cm marking to achieve a catheter-tip position at the i.t. lumbosacral enlargement (~L4–L5). During this time, light tail twitching and a small amount of cerebrospinal fluid efflux from the 18-gauge needle was typically observed indicating successful i.t. catheter placement. Drug or vehicle was injected during a 10 second interval. Drug treatment was randomly assigned to animals. Upon completion of injection, the PE-10 i.t. catheter was removed followed by removal of the 18-gauge needle. A 100% motor recovery rate was observed from this injection procedure.

2.8. Immunohistochemical procedures from CCI-treated rats

Following behavioral assessment, animals were overdosed with an intraperitoneal injection sodium phenobarbital (Sleep away, Fort Dodge Animal Health, Fort Dodge, IA), then perfused transcardially with saline followed by 4% paraformaldehyde. Whole vertebral columns with intact spinal cords (cervical 2 through sacral 1 spinal column segments) were removed, and underwent overnight fixation in 4% paraformaldehyde at 4°C. This tissue collection approach ensured that all relevant anatomical components, including the spinal cord, DRG, and overlying meninges, were intact within the vertebral column, allowing important spatial relationships to remain for examining corresponding functional interactions at individual and specific spinal cord levels. All specimens underwent EDTA (Sigma Aldrich, St. Louis, MO) decalcification for 30 days, and spinal cord sections were subsequently paraffin processed and embedded in ParaplastPlus Embedding Media (McCormick Scientific, St. Louis, MO) as previously described [93]. Adjacent tissue sections (7μm) were mounted on vecta bond-treated slides (Vector Labs, Burlingame, CA), and allowed to adhere to slides overnight at 40°C, followed by deparaffinization, and rehydration via descending alcohols to PBS (1X, pH 7.4). Sections were then processed with microwave antigen retrieval procedures (citrate buffer pH 6.0, or tris-based buffer, pH 9.0; BioCare Medical, Concord, CA).

Slides were incubated with 5% normal donkey serum (NDS), in PBS(pH 7.4) for 2 hours, followed by overnight primary antibody (Table 1) incubation in a humidity chamber at 3° C. Slides underwent secondary antibody incubation (Table 1) for 2 hours in a humidity chamber at room temperature, rinsed in PBS, and then coverslipped with Vectashield containing the nuclear stain 4′,6-diamidino-2-phenylindole (DAPI)(Vector Labs,

NIH-PA Author Manuscript

NIH-PA Author Manuscript

NIH-PA Author Manuscript

Burlingame, CA). For detection of MAGL, phosphorylated p38MAPK, and IL-10 protein, sections were incubated overnight with primary antibodies, incubated with biotinylated secondary antibody (Table 1) for 1 hour, and then treated with Vectastain ABC Elite kit (Vector Labs, Burlingame, CA) and stained using TSA Plus Fluorescein System (PerkinElmer Life Sciences, Waltham, MA) and finally coverslipped with Vectashield containing DAPI. Stained section orientation was kept consistent throughout for proper identification of ipsilateral and contralateral spinal cord and DRGs. For lumbar spinal cord, sections were taken from L4–L6, and the dorsal horn analyzed (Supplemental Fig. 1 *A*). The intact meninges overlying the ipsilateral dorsal horn of the spinal cord were analyzed separately to discern possible immunoreactive changes between surgical and drug treatments groups that may be different from quantified values obtained for the entire ipsilateral dorsal horn. For meningeal analysis, those sections revealing clear identification of the meninges vs. superficial spinal cord were chosen. As such, meninges of tissue sections comprising complete groups stained for IL-10, Iba-1 and MAGL were analyzed. For DRG material, sections were taken containing the DRG corresponding to L5 spinal cord segment, and the most distal portion of the DRG was analyzed (Supplemental Fig. 1 *B*). Low magnification photomicrographs were obtained (Supplemental Fig. 1 *A*, *B*) using a Nikon Optiphot fluorescent microscope equipped with a DP2-BSW (Olympus) camera.

2.9. Confocal microscopy

All tissue processing, slicing, and procedures for immunohistochemistry were identical to that described above. However, in these studies more than one primary antibody was used and examined under confocal microscopy. Therefore, after the first antibody staining procedure, the slides went through subsequent staining procedures. This took place over multiple days to account for the times needed for individual antibody incubation and staining. Confocal microscopy at 63x magnification was then performed on a Zeiss AxioObserver inverted LSM510 META confocal microscope utilizing Zen 2009 software (Carl Zeiss, AG, Germany). Final images were generated from collapsed z-stacks comprised of 17 images taken 0.393 μm apart on the z axis.

2.10. Immunohistochemical spectral image analysis

All images of the spinal cord dorsal horn, overlying meninges and DRGs were captured by a Zeiss Axioscope Microscope, at 20x magnification, with a Nuance Spectral Camera (Cambridge Research & Instrumentation, Woburn, MA). Utilizing the Nuance computer software, the fluorescent wavelength emission spectra range was initially determined for each fluorophoreutilized in the detection of the primary antibody of interest (DAPI, 488 nm +/− 10nm; FITC, 575 nm +/− 5nm; Rhodamine Red 600 nm+/− 5nm) by using a control slide with only a drop of the pure fluorophore. This was performed in the absence of a tissue specimen that may potentially obscure the measurement of the fluorophore's emission spectra. Two sets of additional control slides with tissue sections were prepared, one with only PBS without primary or secondary antibody treatment, and the other without primary but with secondary antibody treatment. These control slides were used to objectively eliminate low intensity fluorescence and autofluorescence background 'noise' from our measurements (Supplemental Fig. 1*C*). Using the control slides, the Nuance software allows the user to set an acceptable threshold of low-level emission fluorescent intensity (as opposed to the software "autothreshold" option) within and outside the defined wavelength range of interest between tissue samples. Emission values that fall below this acceptable threshold of low-level emission, within and outside the defined wavelength range of interest, were eliminated from our measurements (Supplemental Fig. 1 *D*). The fluorescent intensity threshold for each protein marker was determined by the user finding the most appropriate threshold that captures the specific FITC or Rhodamine Red staining for each protein marker within a tissue (e.g., dorsal horn spinal cord or DRG). Once the optimal level of fluorescent

NIH-PA Author Manuscript

NIH-PA Author Manuscript

NIH-PA Author Manuscript

threshold was determined for a particular protein marker, this level was held consistent throughout all of the treatment groups for the image analysis within each protein marker of interest (Supplemental Fig. 1*D*). These steps were followed by software conversion allowing fluorescent wavelength intensity for each fluorophore to be converted to a numerical value. Autofluorescence was defined as that emission outside the defined wavelength of interest (e.g. DAPI, 488 nm +/− 10nm; FITC, 575 nm +/− 5nm; Rhodamine Red 600 nm+/− 5nm) as well as low-level emission that fell below the acceptable threshold of low-level emission fluorescent intensity. These specific autofluorescent and low-level background emission values were subtracted from the image (Supplemental Fig. 1 E,*F*), yielding a numerical value of true fluorescent emission intensity for each fluorophore[44,45].

Primary antibody staining procedures remained consistent to minimize intensity variations of each fluorophore (FITC or Rhodamine Red) used to detect the different primary antibodies of interest. To ensure that fluorophore binding was not impeded through possible steric hindrance of other proximal fluorophores, sections were labeled for only one cellular marker of interest on a slide.

The user also determined the minimum number of connected pixels on the computer screen for image analysis, counted as a region of interest (ROI) defined in the Nuance software system, which resulted in a software image containing distinctive morphology (i.e., of cellular bodies and processes, pattern of protein expression) that was virtually identical to the morphology observed through the microscope for each protein marker. The minimum number of connected pixels would therefore be set higher for a protein expressed abundantly by a cell (i.e., GFAP) in comparison to a protein expressed sparsely, leading to a punctuate pattern (e.g., IL-1β). These conditions resulted in a ROI, and were held consistent for both the ipsilateral and contralateral tissues in every experimental condition and for each antibody stain. The total area of each ROI, as measured by mm^2, is calculated and is factored into the overall measurement of fluorescent intensity per second of exposure. The average count of fluorescent emission intensity per second exposure, per mm^2 is the analyzed value that we report here. That is, fluorescent intensity average count/second/mm^2, which takes into account the density as well as the intensity of the fluorophore detected. A total of 4 sections per animal (N=3) were randomly selected and analyzed in this manner. By applying this novel method of data acquisition and analysis, experimenter bias is eliminated, yielding greater consistency and objectivity to fluorescent quantification.

2.11. Protein quantification by ELISA

Twenty minutes after i.t. gp120 and subsequent behavioral verification, rats were given an overdose i.p. injection (0.8–1.3 cc) of sodium phenobarbital (Sleepaway, Fort Dodge Animal Health, Fort Dodge, IA) and perfused transcardially with ice cold saline followed by exposure of the lumbosacral enlargement by laminectomy. After verifying subdural intrathecal catheter placement and cerebral spinal fluid (CSF) collection, the dorsal portion of the lumbosacral spinal cord and the corresponding bilateral L4-L6 dorsal root ganglia were collected separately into tubes and flash frozen in liquid nitrogen. Tubes were then stored at −80°C until assay. ELISA procedures were performed for IL-1β and TNF-α according to manufacturer's instructions (R&D Systems, Minneapolis, MN).

2.12. Experimental Paradigms

Behavioral efficacy of i.t AM1710 following CCI—Behavioral assessment of BL thresholds was conducted prior to CCI or sham surgical manipulation. Hindpaw threshold responses were assessed 3 and 10 days after surgery. Immediately following behavioral assessment, rats (N=6/group) were given an i.t. injection of AM1710 or vehicle. Hindpaw threshold responses were reassessed during the following 24 hr at discrete time points.

NIH-PA Author Manuscript

NIH-PA Author Manuscript

NIH-PA Author Manuscript

Immunohistochemical detection of spinal and DRG changes—In a separate group of rats (N=3/group), identical BL threshold assessment and surgical procedures were followed, as just described. I.t. AM1710 was injected at the dose (10 ug) identified to produce maximal reversal from allodynia produced by CCI. At the time of maximal efficacy (~3 hr), rats were deeply anesthetized followed by procedures for IHC analysis of tissue sections. Thus, all tissue sections from the dorsal horn of the spinal cord and the corresponding intact DRG were analyzed from behaviorally verified rats from different experimental manipulations (sham vs. CCI + vehicle vs. AM1710).

Behavioral efficacy of i.t AM1710 following i.t. gp120—A separate group of rats were behaviorally verified for BL thresholds followed by chronic i.t. catheterization. Threshold values were reassessed 6 days later. Immediately thereafter, rats received i.t AM1710 or vehicle, and hindpaw threshold responses were reassessed 3 hr later (at maximal AM1710 efficacy). At this time, i.t. gp120 was injected, followed by threshold assessment at 20 min (N=6 rats/group), and immediately followed by anesthetic overdose and tissue collection for protein quantification.

2.13. Data analysis

Psychometric behavioral analysis was performed as previously described[52]to compute the log stiffness that would have resulted in the 50% paw withdrawal rate. Briefly, thresholds were estimated by fitting a Gaussian integral psychometric function to the observed withdrawal rates for each of the tested von Frey hairs, using a maximum-likelihood fitting method [90]. For behavioral statistical analysis to assess the presence of allodynia, a 1-way ANOVA was used at BL, and a 2-way repeated measures ANOVA was used at 3 and 10 days after CCI/sham surgery in CCI-related experiments. To determine AM1710 drug efficacy following i.t. injection on Day 10, a 3-way repeated-measures ANOVA was applied at 0.5, 1, 2, and 2.95 hr timepoints. For experiments utilizing i.t. gp120, a 1-way ANOVA was used at BL, and a 2-way repeated-measures ANOVA was used at 6 days after indwelling catheter surgery, and immediately prior to i.t. gp120. A two-way repeated-measures ANOVA was applied to assess AM1710 efficacy 20 minutes after i.t. gp120. All other data analysis was performed using a one-way ANOVA. A p-value of <0.05 was considered statistically significant. The computer program GraphPad Prism version 4.03 (GraphPad Software Inc., San Diego, CA) was used in all statistical analyses. All data is expressed as mean +/− SEM. For post hoc analysis Bonferroni's test was performed.

3. Results

3.1. Intrathecal injection of AM1710 dose-dependently reverses CCI-induced allodynia

The CB_2R cannabilactone agonist, AM1710, reversed allodynia produced by CCI. Prior to surgical manipulation, all groups exhibited similar bilateral(ipsilateral and contralateral) BL behavioral thresholds (Fig. 1*A,B*). Following CCI, clear *bilateral* allodynia developed by Day 3 and 10 compared to sham-operated rats. On Day 10, following i.t. AM1710 or vehicle injection in sham-operated rats, AM1710 did not alter normal sensory threshold responses to light touch, as well as throughout the entire time course. However, in rats with CCI, i.t. AM1710 produced *reversal* from allodynia, with maximal efficacy observed at 3 hr following the highest dose (10 μg) injected, whereas a 10-fold lower dose (1.0 μg) attenuated allodynia. The lowest dose examined (0.1 μg) did not significantly alter threshold responses, with allodynia remaining stable through the last time point tested (24 hr). All CCI-treated rats revealed full allodynia at 5 hr after i.t. AM1710 treatment.

NIH-PA Author Manuscript

NIH-PA Author Manuscript

NIH-PA Author Manuscript

3.2. Immunohistochemical analysis of spinal cord dorsal horn

Peak behavioral efficacy after i.t. AM1710 injection was again observed at ~ 3 hr compared to neuropathic vehicle-injected rats(Fig. 2 *A,B*), which is in support of the behavioral dose-response characterization above (Fig. 1 *A,B*). Bilateral IL-10 immunoreactivity (IR) in the spinal cord dorsal horn is dramatically decreased in CCI-induced neuropathic rats compared to sham-treated rats (Fig. 2 *C,D*). However, treatment with AM1710 rescued IL-10 IR *bilaterally*, similar to levels found in non-neuropathic controls. The intact meninges surrounding the ipsilateral spinal cord revealed a trend toward decreased IL-10 IR in CCI animals treated with vehicle, however, no changes between treatment groups were observed (Inset, Fig. 2 *C*). Representative fluorescent images of either sham treated with i.t. vehicle (Fig. 2 *K*), CCI treated with i.t. vehicle (Fig. 2 *L*), or with AM1710 (Fig. 2 *M*) corresponding to the quantitative image analysis data are presented. Moreover, confocal microscope examination reveals IL-10 expression in astrocytes (Fig. 6 *C,F*) within superficial (Lam I-II) and deeper dorsal horn laminae (Lam III-V), and microglia (Fig. 6 *I;* Lam I-III). It is notable that when IL-10 returns to non-neuropathic basal levels, allodynia is correspondingly reversed.

For IL-1β IR analysis, compared to non-neuropathic sham-operated rats given i.t. AM1710, or equivolume vehicle, CCI-induced neuropathy produced a robust unilateral increase in IL-1β IR in i.t. vehicle injected animals (Fig. 2 *E,F*). Conversely, i.t. administration of AM1710 completely suppressed increased dorsal horn IL-1β IR. Representative fluorescent images are of sham-treated rats with i.t. vehicle (Fig. 2 *N*), CCI-treated rats with i.t. vehicle (Fig. 2 *O*), or CCI treated-rats with AM1710 injection (Fig. 2 *P*) that correspond to data examined by microscopy analysis. Interestingly, in comparison to IL-10 IR in CCI animals, IL-1β IR observed in the contralateral dorsal spinal cord *was not* substantially elevated when compared to non-neuropathic control animals.

We also examined dorsal horn p-p38 MAPK IR. Compared to sham-operated rats given i.t. AM1710, or equivolume vehicle, CCI-induced neuropathy produced a robust bilateral increase in the dorsal horn of p-p38MAPK IR (Fig. 2 *G,H*). Unexpectedly, AM1710 did not alter ipsilateral or contralateral increases in p-p38MAPK IR. Again, representative fluorescent images are presented, which correspond to image analysis of either sham-treated rats with i.t. vehicle (Fig. 2 *Q*), CCI-treated rats with i.t. vehicle (Fig. 2 *R*), or CCI-treated rats with AM1710 (Fig. 2 *S*).

Upon close examination of the nuclear specific dye, DAPI, no differences in fluorescence intensity as a consequence of either CCI procedures or i.t. drug injections were observed, suggesting that local lumbar cellular numbers remained relatively unchanged (Fig. 2 *I, J*).

While non-neuropathic sham-operated animals given i.t. AM1710 or equivolume vehicle exhibited similar Iba-1 IR levels, a marker for altered microglial activity, AM1710 did not modify the *increased* dorsal horn Iba-1 IR in CCI-treated rats during AM1710-induced reversal from allodynia compared to CCI-treated treated rats with ongoing allodynia (Fig. 3 *A,B*). Therefore, despite robust suppression of dorsal horn IL-1β expression and full reversal of allodynia, local administration of AM1710 does not inhibit increased levels of spinal Iba-1 IR. Meningeal Iba-1 IR was significantly elevated in CCI-treated compared to non-neuropathic sham-treated rats (Fig. 3 *A* Inset). While a trend toward decreased Iba-1 IR was observed in meninges of CCI-treated rats given i.t. AM1710, this decrease was insignificant.

Bilateral dorsal horn GFAP IR expression in adjacent Iba-1 stained sections was examined. Compared to non-neuropathic sham-operated rats given i.t. AM1710, or equivolume vehicle, a robust bilateral increase in dorsal horn GFAP was demonstrated in neuropathic rats (Fig. 3 *C,D*). However, clear suppressive effects of AM1710 on astrocyte activation were observed.

NIH-PA Author Manuscript

NIH-PA Author Manuscript

NIH-PA Author Manuscript

Intrathecal AM1710 strikingly reduced the bilateral increases in dorsal horn GFAP IR seen in CCI vehicle-treated rats (Fig. 3 *C,D*). Corresponding representative fluorescent images used for analysis are shown; sham-operated rats treated with either i.t. vehicle or AM1710 (Fig. 3 *E,F*), or CCI-treated rats injected with either i.t. AM1710 or equivolume vehicle (Fig. 3 *G,H*).

FAAH and MAGL IR were examined at maximal anti-allodynic efficacy of AM1710. Surprisingly, no changes were observed in FAAH IR between non-neuropathic sham and neuropathic CCI rats following i.t. AM1710 or equivolume vehicle (Fig. 4 *A,B*). However, the exact opposite was observed with MAGL IR. That is, neuropathic rats given i.t. vehicle showed a robust bilateral increase in dorsal horn MAGL IR compared to non-neuropathic sham-operated rats given i.t. AM1710, or equivolume vehicle (Fig. 4 *C,D*). These observed MAGL IR increases were robustly and ipsilaterally suppressed in spinal cords of rats treated with i.t. AM1710 (Fig. 4 *C,D*). The intact meninges overlying the ipsilateral spinal cord were also separately analyzed. Different from dorsal spinal analysis, a significant increase in MAGL IR was observed from non-neuropathic sham rats given i.t. AM1710 compared to non-neuropathic rats given i.t. vehicle (Inset, Fig. 4 *C*). Like dorsal spinal analysis, a clear increase in MAGL IR from CCI-treated rats given vehicle was measured. Representative corresponding fluorescent images of analyses from whole dorsal horn spinal cord are shown from sham-operated rats injected with either i.t. vehicle or AM1710 (Fig. 4 *E,F*), or CCI-treated rats with either i.t. vehicle or AM1710 (Fig. 4 *G,H*). While MAGL has been identified in neuronal and microglial cultures, we show that MAGL can be expressed in microglia *in vivo* (Fig. 6 *J,K,L*)

3.3. Immunohistochemical analysis of dorsal root ganglia

Non-neuropathic sham-operated rats given i.t. AM1710, or equivolume vehicle, revealed low GFAP IR, a marker for satellite cells. In striking contrast, a robust bilateral increase in GFAP IR was observed in the DRG from CCI-induced neuropathic rats given i.t. vehicle (Fig. 5 *A,B*). However, AM1710 robustly blocked bilateral GFAP IR increases in DRG (Fig. 5 *A,B*). Ipsilateral, and not contralateral, DRG increases in levels of p-p38MAPK (Fig. 5 *C,D*), IL-1β (Fig. 5 *E,F*) and decreases in IL-10 (Fig. 5 *G,H*) were observed in vehicle injected neuropathic rats. However, following i.t. AM1710, these immunoreactive changes in p-p38MAPK, IL-1β and IL-10 significantly recovered to non-neuropathic controls levels. Representative corresponding p-p38MAPK and IL-10 immunofluorescent images of these analyses are shown from ipsilateral DRG of sham-operated rats treated with i.t. vehicle (Fig. 5 *I,L*), or CCI-treated rats given either i.t. vehicle (Fig. 5 *J,M*) or AM1710 (Fig. 5 *K,N*).

3.4. Identification of IL-10 expressed in dorsal horn astrocytes and microglia

Within the superficial laminae, IL-10 is not co-labeled with GFAP positive cells (Fig. 6 *A,B,C*). However, within the deeper laminae of the dorsal spinal cord, IL-10 is extensively co-labeled with GFAP, (Fig. 6 *D,E,F*) while co-labeling with NF-H (neurons) was completely absent (data not shown). Additionally, Iba-1 positive cells (macrophages and/or resident microglia) express IL-10 protein in laminae I-III (Fig. 6 *G,H,I*).

3.5. Blockade of gp120-induced allodynia and DRG IL-1β production

Pilot data determined the timecourse in which AM1710 blocked the ability of gp120 to induce allodynia. We found that 10 μg of AM1710 was sufficient in blocking the initial development of gp120-induced allodynia, with the anti-allodynic effects gone by 60 minutes (data not shown). All animals revealed similar BL responses prior to i.t. lumbar cannula implantation, i.t. AM1710 or equivolume vehicle injection (Day 6), and immediately prior i.t. gp120 (Fig. 7 *A, B*). As expected, a robust bilateral allodynia was observed in animals given i.t. pretreatment with the vehicle for AM1710 followed ~3 hrs later by i.t. gp120. In

NIH-PA Author Manuscript

NIH-PA Author Manuscript

NIH-PA Author Manuscript

stark contrast, i.t. pretreatment with AM1710 completely prevented the initiation of the bilateral gp120-induced allodynia (Fig. 7 *A, B*). Tissue collected from these animals 20 minutes after gp120 administration revealed a robust increase in IL-1β protein levels and a strong trend toward increased TNF-α protein production in the L4-L6 DRG corresponding to L4-L6 spinal segments exposed to i.t gp120 compared to controls (Fig. 7 *C, D*). However, IL-1β protein was significantly suppressed in animals given i.t. AM1710 pretreatment followed by gp120, while a strong trend toward blunted TNF-α protein production was measured. Expectedly, changes in IL1-β and TNF-α within either the CSF or the dorsal horn spinal cord was not observed at this early post-i.t. gp120 timepoint.

4. Discussion

In this study, we present evidence that a distinct anti-inflammatory response is induced following spinal (i.t.) administration of the recently characterized cannabinoid CB_2R agonist compound from the cannabilactone class, AM1710, which either prevents or reverses allodynia induced in two distinguishable animal models. The findings of each animal model will be discussed in turn. In the CCI model, a transitory bilateral reversal of allodynia from chronic unilateral CCI is observed following i.t. AM1710 administration. While AM1710 was previously shown to increase nociceptive thresholds following peripheral administration in naïve rats [34,68], this study reports that normal light touch sensory thresholds are not altered following i.t. AM1710 in non-neuropathic rats. Additionally, immunoreactivity (IR) for IL-10, significantly decreased in CCI-treated rats. In striking contrast, i.t. AM1710 in CCI neuropathic animals reset bilateral IL-10 IR to basal levels. Overlying meninges revealed similar, albeit insignificant, trends in IL-10. Furthermore, using confocal microscopy, dorsal horn localization of IL-10 is observed in astrocytes and microglia in superficial and deeper laminae (III-V). Together, these findings suggest that spinal parenchyma IL-10 regulate glia to induce pain relief.

It is critical to note that in response to peripheral nerve injury, CNS cellular populations can increase by proliferation of microglia [85], astrocytes [91], or by influx of bone marrow derived perivascular microglia and macrophages [100]. Thus, increased immunoreactivity of specific proteins in the lumbar spinal cord could simply be due to a general increase in cell numbers constitutively expressing these markers. However, DAPI-IR of cellular nuclei remained constant in all experimental conditions, supporting the possibility that cellular specific responses to CCI and AM1710 occurred.

Indeed, alterations in several proinflammatory markers were observed in the spinal cord dorsal horn following CCI. Bilateral increases in p38MAPK IR were observed, supporting prior work demonstrating that p38MAPK plays a critical role in mechanical allodynia that involves the action of proinflammatory cytokines including IL-1β in models of peripheral nerve lesions [62,28,30]. While increased ipsilateral spinal IL-1β mRNA was recently reported following sciatic nerve ligation [78], the current data in this study is the first demonstration of increased unilateral IL-1β IR in anatomically intact spinal cord dorsal horn of rats with CCI-induced allodynia. As with IL-10, AM1710 reset IL-1β to basal levels, but p-p38MAPK remained completely unaltered by AM1710, suggesting that basal levels of IL-10 are not sufficient to suppress activated p-p38MAPK IR. In addition, the data reported here show bilateral increases in GFAP-IR were observed in neuropathic rats. Prior work suggests that increased GFAP expression may not simply be a cellular marker co-incident with neuropathy, as has been frequently reported [18,67,77], but rather, may play a critical role mediating neuropathic pain [35]. Interestingly, CB_2R activation in neuropathic rats resulted in significantly reduced superficial dorsal horn GFAP-IR [72], which may occur via microglial alterations because astrocytes make contact with microglia.

NIH-PA Author Manuscript

NIH-PA Author Manuscript

NIH-PA Author Manuscript

CB_2R expression has been identified mostly in spinal microglia [8,67,69,70,102]. While AM1710 blunted increases in GFAP IR, Iba-1-IR remained unaltered. Iba-1 is one of several immunohistochemical markers used to identify active microglia[1,32]. Spinal cord microglial activation, identified by Iba-1 IHC staining, was reversed by 3 hours following treatment with a microglial-specific inhibitor [88]. Other markers include the CD11b/CD18 [54], or translocator protein (TSPO), formerly known as the peripheral benzodiazepine receptor [10]preferentially expressed in CNS macrophage/microglia. However, in contrast to prior reports revealing decreased microglial activation following i.t. CB_2R activation [69,72,89], we show increased Iba-1-IR persists following i.t. AM1710 and during reversal from allodynia. However, interpretations of these results are limited, given only a single microglial marker was used to examine microglial activation. Nevertheless, microglia produce the anti-inflammatory endocannabinoid,2-arachidonyl glycerol (2-AG) during pathological CNS conditions[83,99]. Notably, microglia may also be a source of IL-10 [59]in the spinal cord. Indeed, co-localization of IL-10 in microglia within superficial and deeper spinal cord laminae (III-IV) in behaviorally reversed CCI-treated rats is shown in this report.

The bioavailability of endocannabinoids such as anandamide and 2-AG produced and released from neurons and microglia [83,94]are primarily controlled through enzymatic metabolism by FAAH and MAGL [3,7,47]. Inhibitors of FAAH and MAGL that result in increased CNS levels of AEA and 2-AG, suppress pathological pain [36,37,42,46]. The current study uniquely shows increased dorsal horn MAGL-IR of neuropathic rats that is reduced following i.t. AM1710 in allodynic-reversed rats. As noted above, microglia are a known source of 2-AG [83], where the actions of MAGL have been described [60]. We additionally show that MAGL expression is co-localized in superficial dorsal horn microglia using confocal microscopy. Interestingly, no change in FAAH-IR was observed.

Satellite glial cells in the DRG form a clear sheath around individual large and small sensory neurons, and when activated under neuropathic conditions, reveal enriched GFAP and IL-1β expression [6,11,35,86,87]. IL-1β released from satellite glia further stimulates sensory neurons. Notably, DRG p-p38MAPK expression is well-characterized following peripheral nerve injury associated with pathological pain [29,101]. Here, examination of DRG revealed increased unilateral p-p38MAPK, IL-1β, and bilateral peri-neuronal (satellite cells) GFAP-IR in neuropathic animals, while i.t. AM1710 abolished all of these changes. Like that observed in spinal cord dorsal horn, DRG IL-10 expression was significantly *diminished* during chronic neuropathy, in support of prior reports [35,36,75], and AM1710 resulted in basal IL-10-IR levels.

Bilateral allodynia induced by unilateral sciatic nerve CCI is demonstrated in this study supporting previous findings [5,15,43,51,55,64,65,82]. Reports demonstrating bilateral biochemical changes in lumbar spinal cord substantiate these behavioral observations. Prior demonstrations include, a decrease in α2-adrenergic receptor mRNA expression [40], greater Fos protein in neurons [73], and IL-6 mRNA upregulation [15]. However, unique findings from the present work reveal unilateral spinal cord dorsal horn IL-1β-IR increases. Thus, the spinal actions of IL-1β must be critical for inducing ipsilateral biochemical changes that in turn alter contralateral spinal cord activity. One possible mechanism may involve ipsilateral IL-1β mediated astrocyte activation that spreads to the contralateral spinal cord via astrocyte gap-junctional communication. Evidence for a critical role of spinal gap-junctional communication leading to contralateral allodynia that is partly mediated by IL-1β has been reported in a model of localized sciatic nerve inflammation [82].

Intrathecal HIV-1 gp120 is an informative model of pathological pain because the spinal actions of IL-1β, p38MAPK and other proinflammatory factors are necessary for allodynia

NIH-PA Author Manuscript

NIH-PA Author Manuscript

NIH-PA Author Manuscript

to develop [24,52–54]. Here, the onset of gp120-induced allodynia replicated previously characterized allodynia [24,52–54,98]. However, an early timepoint analysis of IL1-β reveals no changes in CSF or dorsal horn, in support of prior reports [53,54], while increases in DRG IL1-β are observed. Allodynia and increased protein levels of DRG IL-1β following i.t. HIV-1 gp120 was completely prevented by i.t. AM1710 pretreatment, supporting immunofluorescent quantitative IL-1β changes observed from DRG in CCI neuropathic animals.

CB_2Rs can modulate various signal transduction pathways involved in controlling allodynia in the animal models utilized in this report; CCI and i.t. gp120. While each model initiates spinal glial responses with subsequent proinflammatory cytokine production by different pathways, their downstream intracellular pathways converge. In CCI, enhanced central terminal and dorsal horn neurotransmitter (glutamate, substance P), ATP and chemokine release occurs, activating their cognate receptors on surrounding microglia, astrocytes and neurons [25,31,49,76,97]. Separately, i.t. gp120 activates microglia and astrocytes in their role as immunocompetent cells that release neuroactive substances culminating in allodynia [96]. However, for both models, activated MAPKs, such as extracellular signal-regulated kinases (ERK1/2), p38 and c-Jun N-terminal Kinase (JNK), are critical contributors of glial intracellular signaling leading to IL-1β and TNF-α synthesis and pathological pain [24,28,38,39,48,54]. Additionally, spinal nitric oxide (NO), highly reactive through secondary reactions creating reactive oxygen species, activates MAPKs[81]and mediates allodynia in both models [24,48,98]. CB_2R activation impacts signaling pathways involving cAMP, ERK1/2, JNK, p38-MAPKs and NO production [12,13,16,17]by several potential mechanisms. First, CB_2R activation induces the expression of MAPK phosphatase-1 (MKP-1) in microglial cells, which acts to de-activate ERK1/2 and decrease NO production [16]. Second, CB_2R activation induces IL-10 production [39]that is well-established to suppress IL-1β, TNF-α and NO production [59]. While CB_2R-mediated IL-10 production requires p38-, ERK1/2 and JNK-MAPK activation [13], concurrent inhibition of downstream translocation to the nucleus of the transcription factor, nuclear factor-kappaB (NFkB) that triggers IL-1β and TNF-α transcriptional activation, occurs by disrupting cytoplasmic IkBα important for NFkB translocation [12]. The recently recognized key glial receptor participating in pathological pain, toll-like receptor 4 (TLR4), may become activated not only by its classic ligand, lipopolysaccharaide, but also by factors released from i.t. gp120- or CCI-activated glia and damaged neurons [92,95]. An intriguing possibility is that CB_2R activation may exert anti-inflammatory effects through the ceramide pathway [2], as ceramide analogs and TLR4 activation in microglia act synergistically to produce IL-10 via the p38MAPK pathway [19,20].

Together, the implication of these results is that CB_2R compounds capable of acting on both the spinal cord and DRG glial cytokines can control clinically relevant pathological pain conditions.

Supplementary Material

Refer to Web version on PubMed Central for supplementary material.

Acknowledgments

The authors would like to thank Genevieve Phillips at the University of New Mexico Cancer Center Shared Microscopy Center for her valuable input and training on the spectral software utilized. This work was supported by NIH grants: NIDA 018156, GM60201. This project was also funded in part by the *Dedicated Health Research Funds from the University of New Mexico School of Medicine*.

NIH-PA Author Manuscript

NIH-PA Author Manuscript

NIH-PA Author Manuscript

References

1. Ahmed Z, Shaw G, Sharma VP, Yang C, McGowan E, Dickson DW. Actin-binding proteins coronin-1a and IBA-1 are effective microglial markers for immunohistochemistry. J Histochem Cytochem. 2007; 55:687–700. [PubMed: 17341475]
2. Alpini G, Demorrow S. Changes in the endocannabinoid system may give insight into new and effective treatments for cancer. Vitam Horm. 2009; 81:469–485. [PubMed: 19647123]
3. Basavarajappa BS. Critical enzymes involved in endocannabinoid metabolism. Protein Pept Lett. 2007; 14:237–246. [PubMed: 17346227]
4. Bennett GJ, Xie KY. A peripheral mononeuropathy in rat that produces disorders of pain sensation like those seen in man. Pain. 1988; 33:87–107. [PubMed: 2837713]
5. Bessiere B, Laboureyras E, Chateauraynaud J, Laulin JP, Simonnet G. A single nitrous oxide (N2O) exposure leads to persistent alleviation of neuropathic pain in rats. J Pain. 2009; 11:13–23. [PubMed: 19783223]
6. Binshtok AM, Wang H, Zimmermann K, Amaya F, Vardeh D, Shi L, Brenner GJ, Ji RR, Bean BP, Woolf CJ, Samad TA. Nociceptors are interleukin-1beta sensors. J Neurosci. 2008; 28:14062–14073. [PubMed: 19109489]
7. Blankmann, Jl; Simon, GM.; Cravatt, BF. A comprehensive profile of brain enzymes that hydrolyze the endocannabinoid 2-arachidonoylglycerol. Chem Biol. 2007; 14:1347–1356. [PubMed: 18096503]
8. Cabral GA, Raborn ES, Griffin L, Dennis J, Marciano-Cabral F. CB2 receptors in the brain: role in central immune function. Br J Pharmacol. 2008; 153:240–251. [PubMed: 18037916]
9. Chaplan SR, Bach FW, Pogrel JW, Chung JM, Yaksh TL. Quantitative assessment of tactile allodynia in the rat paw. J Neurosci Meth. 1994; 53:55–63.
10. Chauveau F, Boutin H, Van Camp N, Dolle F, Tavitian B. Nuclear imaging of neuroinflammation: a comprehensive review of [11C] PK11195 challengers. Eur J Nucl Med Mol Imaging. 2008; 35:2304. [PubMed: 18828015]
11. Copray JC, Mantingh I, Brouwer N, Biber K, Kust BM, Liem RS, Huitinga I, Tilders FJ, Van Dam AM, Boddeke HW. Expression of interleukin-1 beta in rat dorsal root ganglia. J Neuroimmunol. 2001; 118:203–211. [PubMed: 11498255]
12. Correa F, Hernangomez M, Mestre L, Loria F, Spagnolo A, Docagne F, Di Marzo V, Guaza C. Anandamide enhances IL-10 production in activated microglia by targeting CB(2) receptors: roles of ERK1/2, JNK, and NF-kappaB. Glia. 2010; 58:135–147. [PubMed: 19565660]
13. Correa F, Mestre L, Docagne F, Guaza C. Activation of cannabinoid CB2 receptor negatively regulates IL-12p40 production in murine macrophages: role of IL-10 and ERK1/2 kinase signaling. Br J Pharmacol. 2005; 145:441–448. [PubMed: 15821753]
14. De Leo, JA.; Sorkin, LS.; Watkins, LR., editors. Immune and Glial Regulation of Pain. IASP Press; Seattle: 2007.
15. Dubovy P, Klusakova I, Svizenska I, Brazda V. Satellite glial cells express IL-6 and corresponding signal-transducing receptors in the dorsal root ganglia of rat neuropathic pain model. Neuron Glia Biol. 2010; 6:73–83. [PubMed: 20519054]
16. Eljaschewitsch E, Witting A, Mawrin C, Lee T, Schmidt PM, Wolf S, Hoertnagl H, Raine CS, Schneider-Stock R, Nitsch R, Ullrich O. The endocannabinoidanandamide protects neurons during CNS inflammation by induction of MKP-1 in microglial cells. Neuron. 2006; 49:67–79. [PubMed: 16387640]
17. Fernandez-Ruiz J, Romero J, Velasco G, Tolon RM, Ramos JA, Guzman M. Cannabinoid CB2 receptor: a new target for controlling neural cell survival? Trends Pharmacol Sci. 2007; 28:39–45. [PubMed: 17141334]
18. Gao YJ, Ji RR. Targeting astrocyte signaling for chronic pain. Neurotherapeutics. 2010; 7:482–493. [PubMed: 20880510]
19. Goldsmith M, Avni D, Ernst O, Glucksam Y, Levy-Rimler G, Meijler MM, Zor T. Synergistic IL-10 induction by LPS and the ceramide-1-phosphate analog PCERA-1 is mediated by the cAMP and p38 MAP kinase pathways. Mol Immunol. 2009; 46:1979–1987. [PubMed: 19362373]

NIH-PA Author Manuscript

NIH-PA Author Manuscript

NIH-PA Author Manuscript

20. Goldsmith M, Avni D, Levy-Rimler G, Mashiach R, Ernst O, Levi M, Webb B, Meijler MM, Gray NS, Rosen H, Zor T. A ceramide-1-phosphate analogue, PCERA-1, simultaneously suppresses tumour necrosis factor-alpha and induces interleukin-10 production in activated macrophages. Immunology. 2009; 127:103–115. [PubMed: 18793216]
21. Guindon J, Hohmann AG. Cannabinoid CB2 receptors: a therapeutic target for the treatment of inflammatory and neuropathic pain. Br J Pharmacol. 2008; 153:319–334. [PubMed: 17994113]
22. Haddad JJ, Saade NE, Safieh-Garabedian B. Interleukin-10 and the regulation of mitogen-activated protein kinases: are these signalling modules targets for the anti-inflammatory action of this cytokine? Cell Signal. 2003; 15:255–267. [PubMed: 12531424]
23. Hanani M. Satellite glial cells in sensory ganglia: from form to function. Brain Res Brain Res Rev. 2005; 48:457–476. [PubMed: 15914252]
24. Holguin A, O'Connor KA, Biedenkapp J, Campisi J, Wieseler-Frank J, Milligan ED, Hansen MK, Spataro L, Maksimova E, Bracmann C, Martin D, Fleshner M, Maier SF, Watkins LR. HIV-1 gp120 stimulates proinflammatory cytokine-mediated pain facilitation via activation of nitric oxide synthase-I (nNOS). Pain. 2004; 110:517–530. [PubMed: 15288392]
25. Inoue K, Koizumi S, Tsuda M. The role of nucleotides in the neuron--glia communication responsible for the brain functions. J Neurochem. 2007; 102:1447–1458. [PubMed: 17697046]
26. Jancalek R, Dubovy P, Svizenska I, Klusakova I. Bilateral changes of TNF-alpha and IL-10 protein in the lumbar and cervical dorsal root ganglia following a unilateral chronic constriction injury of the sciatic nerve. J Neuroinflammation. 2010; 7:11. [PubMed: 20146792]
27. Jancalek R, Svizenska I, Klusakova I, Dubovy P. Bilateral changes of IL-10 protein in lumbar and cervical dorsal root ganglia following proximal and distal chronic constriction injury of peripheral nerve. Neurosci Lett. 2011; 501:86–91. [PubMed: 21763399]
28. Ji RR, Gereau RWt, Malcangio M, Strichartz GR. MAP kinase and pain. Brain Res Rev. 2009; 60:135–148. [PubMed: 19150373]
29. Ji RR, Samad TA, Jin SX, Schmoll R, Woolf CJ. p38 MAPK activation by NGF in primary sensory neurons after inflammation increases TRPV1 levels and maintains heat hyperalgesia. Neuron. 2002; 36:57–68. [PubMed: 12367506]
30. Ji RR, Suter MR. p38 MAPK, microglial signaling, and neuropathic pain. Mol Pain. 2007; 3:33. [PubMed: 17974036]
31. Jung H, Toth PT, White FA, Miller RJ. Monocyte chemoattractant protein-1 functions as a neuromodulator in dorsal root ganglia neurons. J Neurochem. 2008; 104:254–263. [PubMed: 17944871]
32. Kanazawa H, Ohsawa K, Sasaki Y, Kohsaka S, Imai Y. Macrophage/microglia-specific protein Iba1 enhances membrane ruffling and Rac activation via phospholipase C-gamma-dependent pathway. J Biol Chem. 2002; 277:20026–20032. [PubMed: 11916959]
33. Kawasaki Y, Zhang L, Cheng J-K, Ji R-R. Cytokine mechanisms of central sensitization: Distinct and overlapping role of interleukin-1b, interleukin-6, and tumor necrosis factor-a in regulating syntapic and neuronal activity in the superficial spinal cord. J Neurosci. 2008; 28:5189–5194. [PubMed: 18480275]
34. Khanolkar AD, Lu D, Ibrahim M, Duclos RI Jr, Thakur GA, Malan TP Jr, Porreca F, Veerappan V, Tian X, George C, Parrish DA, Papahatjis DP, Makriyannis A. Cannabilactones: a novel class of CB2 selective agonists with peripheral analgesic activity. J Med Chem. 2007; 50:6493–6500. [PubMed: 18038967]
35. Kim DS, Figueroa KW, Li KW, Boroujerdi A, Yolo T, Luo ZD. Profiling of dynamically changed gene expression in dorsal root ganglia post peripheral nerve injury and a critical role of injury-induced glial fibrillary acidic protein in maintenance of pain behaviors [corrected]. Pain. 2009; 143:114–122. [PubMed: 19307059]
36. Kinsey SG, Long JZ, Cravatt BF, Lichtman AH. Fatty acid amide hydrolase and monoacylglycerol lipase inhibitors produce anti-allodynic effects in mice through distinct cannabinoid receptor mechanisms. J Pain. 2010; 11:1420–1428. [PubMed: 20554481]
37. Kinsey SG, Long JZ, O'Neal ST, Abdullah RA, Poklis JL, Boger DL, Cravatt BF, Lichtman AH. Blockade of endocannabinoid-degrading enzymes attenuates neuropathic pain. J Pharmacol Exp Ther. 2009; 330:902–910. [PubMed: 19502530]

NIH-PA Author Manuscript

NIH-PA Author Manuscript

NIH-PA Author Manuscript

38. Lee C, Liu QH, Tomkowicz B, Yi Y, Freedman BD, Collman RG. Macrophage activation through CCR5- and CXCR4-mediated gp120-elicited signaling pathways. J Leukoc Biol. 2003; 74:676–682. [PubMed: 12960231]
39. Lee C, Tomkowicz B, Freedman BD, Collman RG. HIV-1 gp120-induced TNF-{alpha} production by primary human macrophages is mediated by phosphatidylinositol-3 (PI-3) kinase and mitogen-activated protein (MAP) kinase pathways. J Leukoc Biol. 2005; 78:1016–1023. [PubMed: 16081599]
40. Leiphart JW, Dills CV, Levy RM. Decreased spinal alpha2a- and alpha2c-adrenergic receptor subtype mRNA in a rat model of neuropathic pain. Neurosci Lett. 2003; 349:5–8. [PubMed: 12946573]
41. Lever IJ, Robinson M, Cibelli M, Paule C, Santha P, Yee L, Hunt SP, Cravatt BF, Elphick MR, Nagy I, Rice AS. Localization of the endocannabinoid-degrading enzyme fatty acid amide hydrolase in rat dorsal root ganglion cells and its regulation after peripheral nerve injury. J Neurosci. 2009; 29:3766–3780. [PubMed: 19321773]
42. Long JZ, Nomura DK, Vann RE, Walentiny M, Booker L, Jin X, Burston JJ, Sim-Selley LJ, Lichtman AH, Wiley JL, Cravatt BF. Dual blockade of FAAH and MAGL identifies behavioral processes regulated by endocannabinoid crosstalk in vivo. Proc Natl Acad Sci U S A. 2009; 106:20270–20275. [PubMed: 19918051]
43. Loram LC, Harrison JA, Sloane EM, Hutchinson MR, Sholar P, Taylor FR, Berkelhammer D, Coats BD, Poole S, Milligan ED, Maier SF, Rieger J, Watkins LR. Enduring reversal of neuropathic pain by a single intrathecal injection of adenosine 2A receptor agonists: a novel therapy for neuropathic pain. J Neurosci. 2009; 29:14015–14025. [PubMed: 19890011]
44. Mahad DJ, Ziabreva I, Campbell G, Laulund F, Murphy JL, Reeve AK, Greaves L, Smith KJ, Turnbull DM. Detection of cytochrome c oxidase activity and mitochondrial proteins in single cells. J Neurosci Methods. 2009; 184:310–319. [PubMed: 19723540]
45. Mansfield JR, Hoyt C, Levenson RM. Visualization of microscopy-based spectral imaging data from multi-label tissue sections. Curr Protoc Mol Biol. 2008; Chapter 14(Unit 14–19)
46. Martin WJ, Loo CM, Basbaum AI. Spinal cannabinoids are anti-allodynic in rats with persistent inflammation. Pain. 1999; 82:199–205. [PubMed: 10467924]
47. McKinney MK, Cravatt BF. Structure and function of fatty acid amide hydrolase. Annu Rev Biochem. 2005; 74:411–432. [PubMed: 15952893]
48. McMahon SB, Cafferty WBJ, Marchand F. Immune and glial cell factors as pain mediators and modulators. Exp Neurol. 2005; 192:444–462. [PubMed: 15755561]
49. McMahon SB, Malcangio M. Current challenges in glia-pain biology. Neuron. 2009; 64:46–54. [PubMed: 19840548]
50. Milligan ED, Hinde JL, Mehmert KK, Maier SF, Watkins LR. A method for increasing the viability of the external portion of lumbar catheters placed in the spinal subarachnoid space of rats. J Neurosci Methods. 1999; 90:81–86. [PubMed: 10517276]
51. Milligan ED, Langer SJ, Sloane EM, He L, Wieseler-Frank J, O'Connor KA, Martin D, Forsayeth JR, Maier SF, Johnson K, Chavez RA, Leinwand LA, Watkins LR. Controlling pathological pain by adenovirally driven spinal production of the anti-inflammatory cytokine, Interleukin-10. European Journal Neuroscience. 2005; 21:2136–2148.
52. Milligan ED, Mehmert KK, Hinde JL, Harvey LOJ, Martin D, Tracey KJ, Maier SF, Watkins LR. Thermal hyperalgesia and mechanical allodynia produced by intrathecal administration of the Human Immunodeficiency Virus-1 (HIV-1) envelope glycoprotein, gp120. Brain Res. 2000; 861:105–116. [PubMed: 10751570]
53. Milligan ED, O'Connor KA, Armstrong CB, Hansen MK, Martin D, Tracey KJ, Maier SF, Watkins LR. Systemic administration of CNI-1493, a p38 mitogen-activated protein kinase inhibitor, blocks intrathecal human immunodeficiency virus-1 gp120-induced enhanced pain states in rats. J Pain. 2001; 2:326–333. [PubMed: 14622812]
54. Milligan ED, O'Connor KA, Nguyen KT, Armstrong CB, Twining C, Gaykema RP, Holguin A, Martin D, Maier SF, Watkins LR. Intrathecal HIV-1 envelope glycoprotein gp120 induces enhanced pain states mediated by spinal cord proinflammatory cytokines. J Neurosci. 2001; 21:2808–2819. [PubMed: 11306633]

NIH-PA Author Manuscript

NIH-PA Author Manuscript

NIH-PA Author Manuscript

55. Milligan ED, Sloane EM, Langer SJ, Cruz PE, Chacur M, Spataro L, Wieseler-Frank J, Hammack SE, Maier SF, Flotte TR, Forsayeth JR, Leinwand LA, Chavez RA, Watkins LR. Controlling neuropathic pain by adeno-associated virus driven production of the anti-inflammatory cytokine, interleukin-10. Molecular Pain. 2005; 1:9–22. [PubMed: 15813997]
56. Milligan ED, Sloane EM, Langer SJ, Hughes TR, Jekich BM, Frank MG, Mahoney JH, Levkoff LH, Maier SF, Cruz PE, Flotte TR, Johnson KW, Mahoney MM, Chavez RA, Leinwand LA, Watkins LR. Repeated intrathecal injections of plasmid DNA encoding interleukin-10 produce prolonged reversal of neuropathic pain. Pain. 2006; 126:294–308. [PubMed: 16949747]
57. Milligan ED, Zapata V, Schoeniger D, Chacur M, Green P, Poole S, Martin D, Maier SF, Watkins LR. An initial investigation of spinal mechanisms underlying pain enhancement induced by fractalkine, a neuronally released chemokine. Eur J Neurosci. 2005; 22:2775–2782. [PubMed: 16324111]
58. Mitrirattanakul S, Ramakul N, Guerrero AV, Matsuka Y, Ono T, Iwase H, Mackie K, Faull KF, Spigelman I. Site-specific increases in peripheral cannabinoid receptors and their endogenous ligands in a model of neuropathic pain. Pain. 2006; 126:102–114. [PubMed: 16844297]
59. Moore KW, de Waal Malefyt R, Coffman RL, O'Garra A. Interleukin-10 and the interleukin-10 receptor. Annu Rev Immunol. 2001; 19:683–765. [PubMed: 11244051]
60. Muccioli GG, Xu C, Odah E, Cudaback E, Cisneros JA, Lambert DM, Lopez Rodriguez ML, Bajjalieh S, Stella N. Identification of a novel endocannabinoid-hydrolyzing enzyme expressed by microglial cells. J Neurosci. 2007; 27:2883–2889. [PubMed: 17360910]
61. Mukherjee S, Adams M, Whiteaker K, Daza A, Kage K, Cassar S, Meyer M, Yao BB. Species comparison and pharmacological characterization of rat and human CB2 cannabinoid receptors. Eur J Pharmacol. 2004; 505:1–9. [PubMed: 15556131]
62. Obata K, Yamanaka H, Kobayashi K, Dai Y, Mizushima T, Katsura H, Fukuoka T, Tokunaga A, Noguchi K. Role of mitogen-activated protein kinase activation in injured and intact primary afferent neurons for mechanical and heat hypersensitivity after spinal nerve ligation. J Neurosci. 2004; 24:10211–10222. [PubMed: 15537893]
63. Otoshi K, Kikuchi S, Konno S, Sekiguchi M. The reactions of glial cells and endoneurial macrophages in the dorsal root ganglion and their contribution to pain-related behavior after application of nucleus pulposus onto the nerve root in rats. Spine (Phila Pa 1976). 2010; 35:264–27.1. [PubMed: 20075775]
64. Paulson PE, Casey KL, Morrow TJ. Long-term changes in behavior and regional cerebral blood flow associated with painful peripheral monotherapy in the rat. Pain. 2002; 95:31–40. [PubMed: 11790465]
65. Paulson PE, Morrow TJ, Casey KL. Bilateral behavioral and regional cerebral blood flow changes during painful peripheral mononeuropathy in the rat. Pain. 2000; 84:233–245. [PubMed: 10666528]
66. Racz I, Nadal X, Alferink J, Banos JE, Rehnelt J, Martin M, Pintado B, Gutierrez-Adan A, Sanguino E, Bellora N, Manzanares J, Zimmer A, Maldonado R. Interferon-gamma is a critical modulator of CB(2) cannabinoid receptor signaling during neuropathic pain. J Neurosci. 2008a; 28:12136–12145. [PubMed: 19005078]
67. Racz I, Nadal X, Alferink J, Banos JE, Rehnelt J, Martin M, Pintado B, Gutierrez-Adan A, Sanguino E, Manzanares J, Zimmer A, Maldonado R. Crucial role of CB(2) cannabinoid receptor in the regulation of central immune responses during neuropathic pain. J Neurosci. 2008b; 28:12125–12135. [PubMed: 19005077]
68. Rahn EJ, Thakur GA, Wood JA, Zvonok AM, Makriyannis A, Hohmann AG. Pharmacological characterization of AM1710, a putative cannabinoid CB(2) agonist from the cannabilactone class: Antinociception without central nervous system side-effects. Pharmacol Biochem Behav. 2011; 98:493–502. [PubMed: 21382397]
69. Romero-Sandoval A, Eisenach JC. Spinal cannabinoid receptor type 2 activation reduces hypersensitivity and spinal cord glial activation after paw incision. Anesthesiology. 2007; 106:787–794. [PubMed: 17413917]
70. Romero-Sandoval A, Nutile-McMenemy N, DeLeo JA. Spinal microglial and perivascular cell cannabinoid receptor type 2 activation reduces behavioral hypersensitivity without tolerance after peripheral nerve injury. Anesthesiology. 2008; 108:722–734. [PubMed: 18362605]

NIH-PA Author Manuscript

NIH-PA Author Manuscript

NIH-PA Author Manuscript

71. Romero-Sandoval EA, Horvath RJ, Deleo JA. Neuroimmune interactions and pain: Focus on glial-modulating targets. Curr Opin Investig Drugs. 2008; 9:726–734.
72. Romero-Sandoval EA, Horvath R, Landry RP, DeLeo JA. Cannabinoid receptor type 2 activation induces a microglial anti-inflammatory phenotype and reduces migration via MKP induction and ERK dephosphorylation. Mol Pain. 2009; 5:25. [PubMed: 19476641]
73. Ro LS, Li HY, Huang KF, Chen ST. Territorial and extra-territorial distribution of Fos protein in the lumbar spinal dorsal horn neurons in rats with chronic constriction nerve injuries. Brain Res. 2004; 1004:177–187. [PubMed: 15033433]
74. Sacerdote P, Massi P, Panerai AE, Parolaro D. In vivo and in vitro treatment with the synthetic cannabinoid CP55, 940 decreases the in vitro migration of macrophages in the rat: involvement of both CB1 and CB2 receptors. J Neuroimmunol. 2000; 109:155–163. [PubMed: 10996217]
75. Schafers M, Geis C, Svensson CI, Luo ZD, Sommer C. Selective increase of tumour necrosis factor-alpha in injured and spared myelinated primary afferents after chronic constrictive injury of rat sciatic nerve. Eur J Neurosci. 2003; 17:791–804. [PubMed: 12603269]
76. Scholz J, Woolf CJ. The neuropathic pain triad: neurons, immune cells, and glia. Nat Neuroscience. 2007; 10:1361–1368.
77. Schreiber KL, Beitz AJ, Wilcox GL. Activation of spinal microglia in a murine model of peripheral inflammation-induced, long-lasting contralateral allodynia. Neurosci Lett. 2008; 440:63–67. [PubMed: 18541374]
78. Shi XQ, Lim TKY, Lee S, Zhao YQ, Zhang J. Statins alleviate experimental nerve injury-induced neuropathic pain. Pain. 2011; 152:1033–1043. [PubMed: 21414721]
79. Siemionow K, Klimczak A, Brzezicki G, Siemionow M, McLain RF. The effects of inflammation on glial fibrillary acidic protein expression in satellite cells of the dorsal root ganglion. Spine (Phila Pa 1976). 2009; 34:1631–1637. [PubMed: 19770604]
80. Skoff AM, Zhao C, Adler JE. Interleukin-1alpha regulates substance P expression and release in adult sensory neurons. Exp Neurol. 2009; 217:395–400. [PubMed: 19341730]
81. Son Y, Cheong YK, Kim NH, Chung HT, Kang DG, Pae HO. Mitogen-Activated Protein Kinases and Reactive Oxygen Species: How Can ROS Activate MAPK Pathways? J Signal Transduct. 2011:792639. [PubMed: 21637379]
82. Spataro LE, Sloane EM, Milligan ED, Wieseler-Frank J, Schoeniger D, Jekich BM, Barrientos RM, Maier SF, Watkins LR. Spinal gap junctions: potential involvement in pain facilitation. J Pain. 2004; 5:392–405. [PubMed: 15501197]
83. Stella N. Endocannabinoid signaling in microglial cells. Neuropharmacology. 2009; 56 (Suppl 1): 244–253. [PubMed: 18722389]
84. Stella N, Schweitzer P, Piomelli D. A second endogenous cannabinoid that modulates long-term potentiation. Nature. 1997; 388:773–778. [PubMed: 9285589]
85. Suter MR, Berta T, Gao YJ, Decosterd I, Ji RR. Large A-fiber activity is required for microglial proliferation and p38 MAPK activation in the spinal cord: different effects of resiniferatoxin and bupivacaine on spinal microglial changes after spared nerve injury. Mol Pain. 2009; 5:53. [PubMed: 19772627]
86. Takeda M, Takahashi M, Matsumoto S. Contribution of activated interleukin receptors in trigeminal ganglion neurons to hyperalgesia via satellite glial interleukin-1beta paracrine mechanism. Brain Behav Immun. 2008; 22:1016–1023. [PubMed: 18440198]
87. Takeda M, Takahashi M, Matsumoto S. Contribution of the activation of satellite glia in sensory ganglia to pathological pain. Neurosci Biobehav Rev. 2009; 33:784–792. [PubMed: 19167424]
88. Talbot S, Chahmi E, Dias JP, Couture R. Key role for spinal dorsal horn microglial kinin B1 receptor in early diabetic pain neuropathy. J Neuroinflammation. 2010; 7:36. [PubMed: 20587056]
89. Toth CC, Jedrzejewski NM, Ellis CL, Frey WH 2nd. Cannabinoid-mediated modulation of neuropathic pain and microglial accumulation in a model of murine type I diabetic peripheral neuropathic pain. Mol Pain. 2010; 6:16. [PubMed: 20236533]
90. Treutwein B, Strasburger H. Fitting the psychometric function. Percept Psychophys. 1999; 61:87–106. [PubMed: 10070202]

NIH-PA Author Manuscript

NIH-PA Author Manuscript

NIH-PA Author Manuscript

91. Tsuda M, Kohro Y, Yano T, Tsujikawa T, Kitano J, Tozaki-Saitoh H, Koyanagi S, Ohdo S, Ji RR, Salter M, Inoue K. JAK-STAT3 pathway regulates spinal astrocyte proliferation and neuropathic pain maintenance in rats. Brain. 2011; 134:1127–1139. [PubMed: 21371995]
92. van Noort JM. Stress proteins in CNS inflammation. J Pathol. 2008; 214:267–275. [PubMed: 18161755]
93. Wallace JA, Romero AA, Gabaldon AM, Roe VA, Saavedra SL, Lobner J. Tyrosine hydroxylase-containing neurons in the spinal cord of the chicken. I. Development and analysis of catecholamine synthesis capabilities. Cell Mol Neurobiol. 1996; 16:625–648. [PubMed: 9013027]
94. Walter L, Franklin A, Witting A, Wade C, Xie Y, Kunos G, Mackie K, Stella N. Nonpsychotropic cannabinoid receptors regulate microglial cell migration. J Neurosci. 2003; 23:1398–1405. [PubMed: 12598628]
95. Watkins LR, Hutchinson MR, Rice KC, Maier SF. The “toll” of opioid-induced glial activation: improving the clinical efficacy of opioids by targeting glia. Trends Pharmacol Sci. 2009; 30:581–591. [PubMed: 19762094]
96. Watkins LR, Milligan ED, Maier SF. Glial activation: a driving force for pathological pain. Trends in Neuroscience. 2001; 24:450–455.
97. White FA, Jung H, Miller RJ. Chemokines and the pathophysiology of neuropathic pain. Proc Natl Acad Sci U S A. 2007; 104:20151–20158. [PubMed: 18083844]
98. Wieseler-Frank J, Jekich BM, Mahoney JH, Bland ST, Maier SF, Watkins LR. A novel immune-to-CNS communication pathway: cells of the meninges surrounding the spinal cord CSF space produce proinflammatory cytokines in response to an inflammatory stimulus. Brain Behav Immun. 2007; 21:711–718. [PubMed: 16989980]
99. Witting A, Walter L, Wacker J, Moller T, Stella N. P2X7 receptors control 2-arachidonoylglycerol production by microglial cells. Proc Natl Acad Sci U S A. 2004; 101:3214–3219. [PubMed: 14976257]
100. Xu H, Chen M, Mayer EJ, Forrester JV, Dick AD. Turnover of resident retinal microglia in the normal adult mouse. Glia. 2007; 55:189–198. [PubMed: 17078023]
101. Xu JT, Xin WJ, Wei XH, Wu CY, Ge YX, Liu YL, Zang Y, Zhang T, Li YY, Liu XG. p38 activation in uninjured primary afferent neurons and in spinal microglia contributes to the development of neuropathic pain induced by selective motor fiber injury. Exp Neurol. 2007; 204:355–365. [PubMed: 17258708]
102. Zhang J, Hoffert C, Vu HK, Groblewski T, Ahmad S, O’Donnell D. Induction of CB2 receptor expression in the rat spinal cord of neuropathic but not inflammatory chronic pain models. Eur J Neurosci. 2003; 17:2750–2754. [PubMed: 12823482]

NIH-PA Author Manuscript
NIH-PA Author Manuscript
NIH-PA Author Manuscript

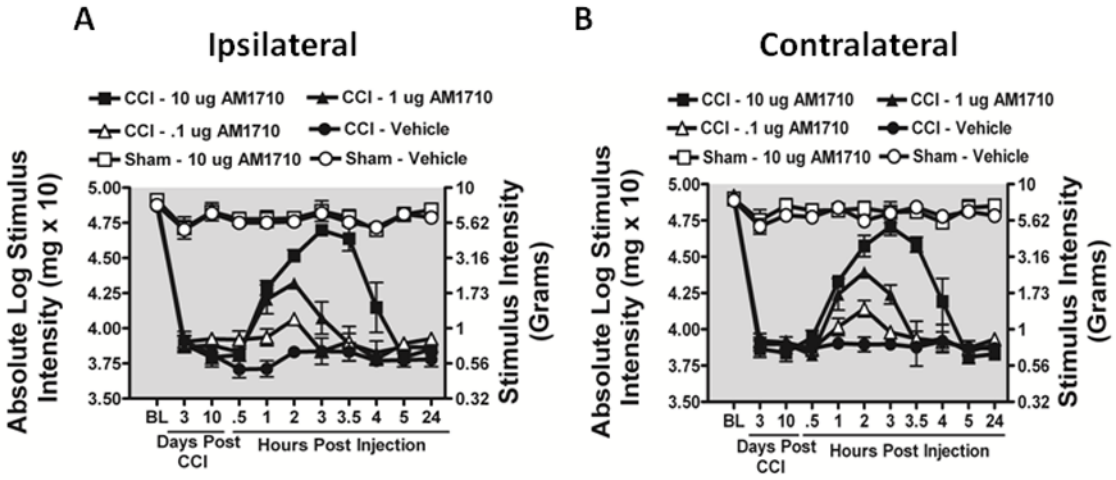

Figure 1.

Selective i.t. cannabinoid 2 receptor agonist AM1710 reverses CCI-induced allodynia. **A**, **B**, AM1710 reverses CCI-induced allodynia in a dose-dependent manner. A total of 36 animals were used in this experiment. Prior to surgical manipulation, all groups exhibited similar bilateral (ipsilateral and contralateral) BL thresholds (ANOVA, $F_{(5,35)}$ =1.982 ; p=0.1124, ANOVA, $F_{(5,35)}$ =1.142; p=0.3616, respectively). Following CCI, clear *bilateral* allodynia developed by Day 3 and continued chronically through Day 10 compared to sham-operated rats. On Day 10, compared to i.t. control injected rats, AM1710 produced a dose-dependent reversal from allodynia, with maximal reversal observed at 3 hours following the highest injected dose (10 μg). However, allodynia fully returned by 5 hours after i.t. AM1710 treatment, with allodynia remaining stable through 24 hours (ipsilateral paw ANOVA, $F_{(15,84)}$ = 187.6; p<0.0001; and contralateral paw, ANOVA, $F_{(15,84)}$=403.7; p<0.0001). While 1.0 μg produced attenuated allodynia, 0.1 μg did not alter allodynia for either the ipsilateral or contralateral hindpaws. Post hoc analysis revealed that 1μg AM1710 produced a robust reversal from allodynia at 2 hours following i.t. injection, while all AM1710 treated animals returned to allodynia by 4 hours (p<0.001).

NIH-PA Author Manuscript
NIH-PA Author Manuscript
NIH-PA Author Manuscript

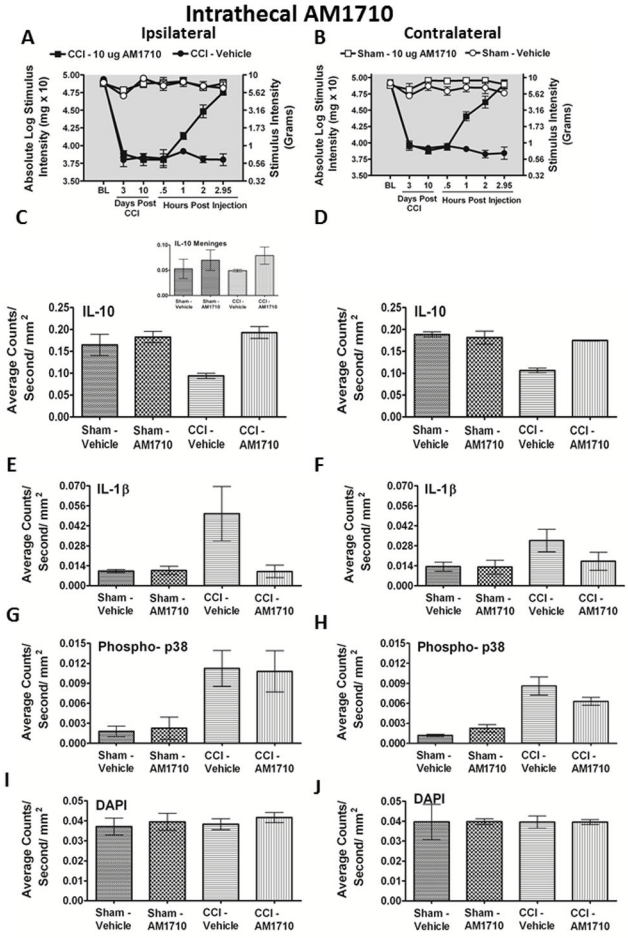

NIH-PA Author Manuscript
NIH-PA Author Manuscript
NIH-PA Author Manuscript

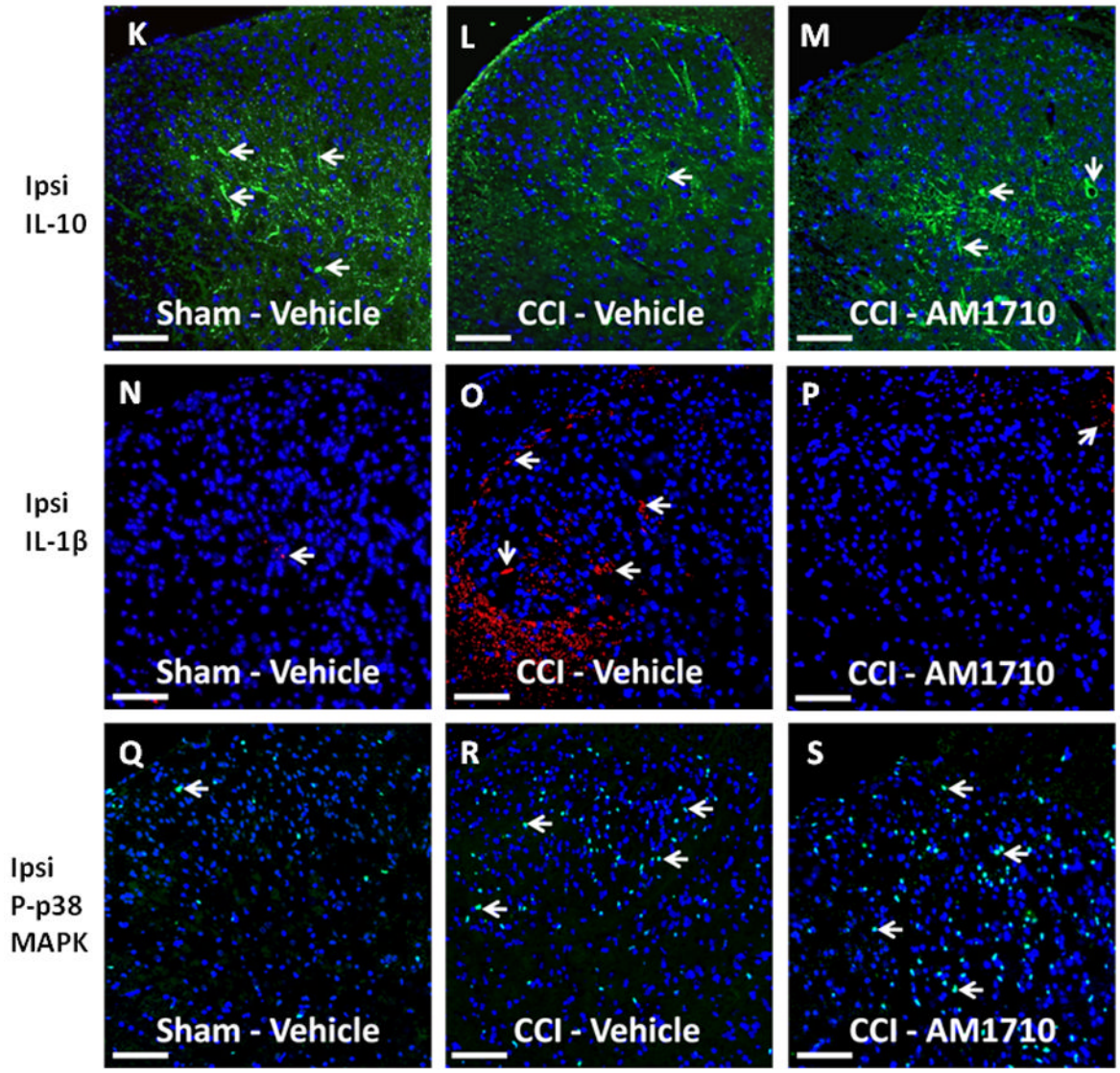

Figure 2.

Immunofluorescent intensity quantification following AM1710 –induced reversal of allodynia. A total of 12 animals were used for both the behavioral experiment reported here and tissues from these animals were analyzed in the reported immunohistochemical experiments. **A**,**B**, Prior to CCI, all groups exhibited similar ipsilateral and contralateral BL thresholds (ANOVA, $F_{(3,11)}$ =2.396; p=0.1438, and ANOVA, $F_{(3,11)}$ =1.432; p=0.3036, respectively). CCI produced significant bilateral allodynia at Day 3 and continued to Day 10 compared to sham-treated animals (ANOVA, $F_{(1,8)}$ =284.8; p< 0.0001, and ANOVA, $F_{(1,8)}$=222.9; p=0.0001, respectively). Behavioral responses following i.t. AM1710 (10 μg) produced maximal bilateral reversal of allodynia (ANOVA, $F_{(1,8)}$= 269.7; p<0.0001 and ANOVA, $F_{(1,8)}$=146.0; p<0.0001, respectively). At peak reversal, animals were sacrificed and spinal tissue was collected. **C**, **D**, Bilateral IL-10-immunoreactivity (IR) in the dorsal horn spinal cord was dramatically decreased in CCI-induced neuropathic rats compared to sham-treated rats. In stark contrast, treatment with AM1710 rescued IL-10 IR to basal levels in both the ipsilateral and contralateral dorsal spinal cord (ANOVA, $F_{(3,11)}$=12.36; p=0.0023; ANOVA, $F_{(3,11)}$=30.68; p<0.0001, respectively). **Inset, C,** No changes in

NIH-PA Author Manuscript

NIH-PA Author Manuscript

NIH-PA Author Manuscript

expression of meningeal IL-10 IR between non-neuropathic sham and neuropathic CCI rats following i.t. AM1710 or equivolume vehicle were observed (ANOVA, $F_{(3,11)}$=1.109; p=0.4008). **E, F,** Compared to non-neuropathic sham-operated rats given i.t. AM1710 or equivolume vehicle, CCI-induced neuropathy produced a robust unilateral increase in IL-1β IR in i.t. vehicle injected animals. Conversely, i.t. administration of AM1710 reversed increased dorsal horn spinal IL-1β IR. IL-1β IR observed in the contralateral dorsal horn spinal cord was not substantially elevated when compared to non-neuropathic control animals. (ANOVA, $F_{(3,11)}$= 6.240; p=0.0172; ANOVA, $F_{(3,11)}$=3.354; p=0.0.760, respectively). **G, H**, Compared to non-neuropathic sham-operated rats given i.t. AM1710 or equivolume vehicle, CCI-induced neuropathy produced a robust p-p38MAPK bilateral IR increase in dorsal horn spinal cord tissues following i.t. vehicle injection. AM1710 administered i.t. did not reverse CCI-induced increases in p38MAPK IR. (ANOVA, $F_{(3,11)}$=4.221; p=0.0459; ANOVA, $F_{(3,11)}$=22.26; p=0.0003, respectively). **I**, **J**, No differences in DAPI nuclear stain fluorescent intensity were observed in AM1710 ipsilateral or contralateral dorsal horn (ANOVA, $F_{(3,11)}$=0.4571; p=0.7197, ANOVA, $F_{(3,11)}$=0.0006230; p=1.0, respectively). **K, L, M,** Representative spectrally unmixed images at 20x magnification of IL-10 fluorescent staining (green) with DAPI nuclear stain (blue). **N, O, P**, Representative spectrally unmixed images at 20x magnification of IL1β fluorescent staining (red) and DAPI nuclear stain (blue). **Q**, **R**, **S**, Representative spectrally unmixed images at 20x magnification of phospho-p38 fluorescent staining (green) with DAPI nuclear stain (blue). In all images the scale bar is equal to 50 μm.

NIH-PA Author Manuscript
NIH-PA Author Manuscript
NIH-PA Author Manuscript

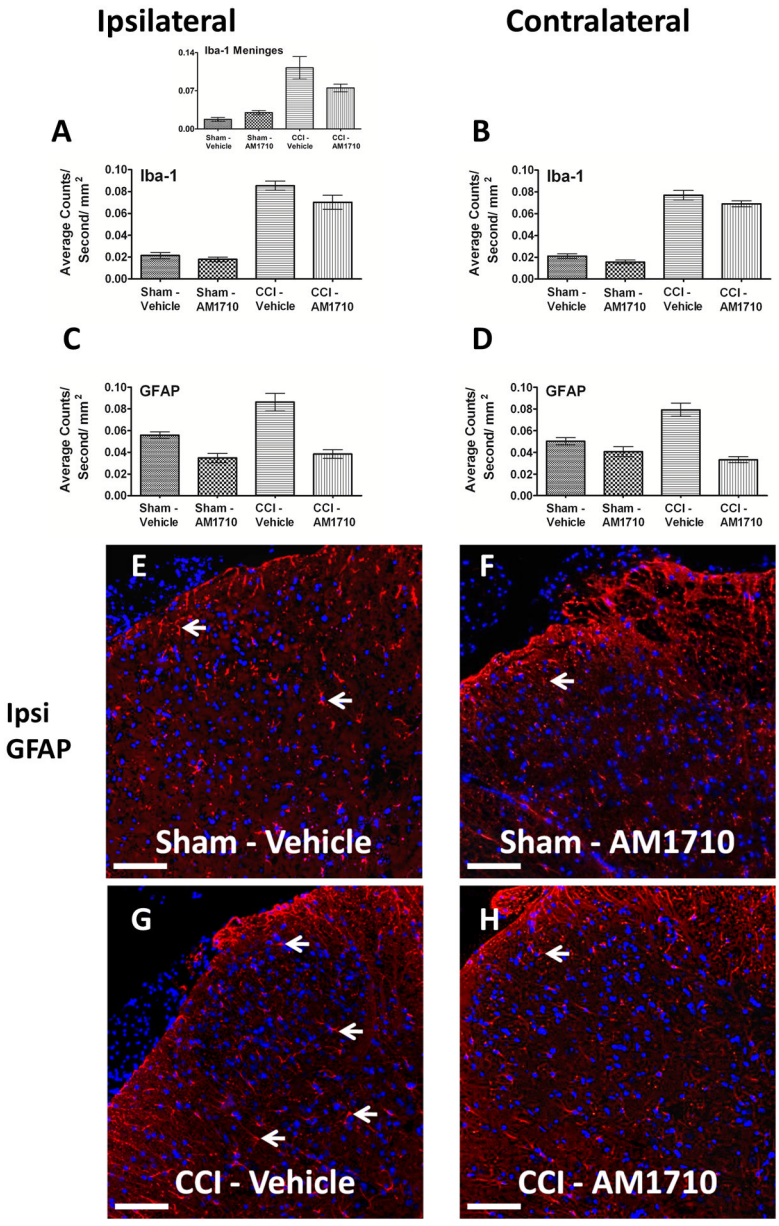

Figure 3.

Immunofluorescent intensity quantification of the spinal cord dorsal horn reveals differences in astrocyte but not microglial activation in neuropathic rats treated with AM1710. **A**, **B**, Compared to non-neuropathic sham-operated rats given i.t. AM1710 or equivolume vehicle, CCI-induced neuropathy produced a robust bilateral increase in spinal cord dorsal horn Iba-1 IR in rats given i.t. vehicle (ANOVA, $F_{(3,11)}=58.94$; $p<0.0001$, ANOVA, $F_{(3,11)}=175.5$; $p<0.0001$, respectively). **Inset, A,** significant changes in expression of meningeal Iba-1 IR between non-neuropathic sham and neuropathic CCI rats following i.t. AM1710 or equivolume vehicle were observed (ANOVA, $F_{(3,11)}=22.55$; $p=0.0003$). **C**, **D**, Compared to non-neuropathic sham-operated rats given i.t. AM1710 or equivolume vehicle, neuropathic rats demonstrated a robust bilateral increase in dorsal horn GFAP IR given i.t. vehicle (ANOVA, $F_{(3,11)}=30.32$; $p=0.0001$, ANOVA, $F_{(3,11)}=31.57$; $p<0.001$, respectively). **E**, **F**, **G**, **H**, Representative spectrally unmixed images at 20x magnification of GFAP

fluorescent staining (red) and DAPI nuclear stain(blue). In all images the scale bar is equal to 50 μm.

NIH-PA Author Manuscript
NIH-PA Author Manuscript
NIH-PA Author Manuscript

NIH-PA Author Manuscript
NIH-PA Author Manuscript
NIH-PA Author Manuscript

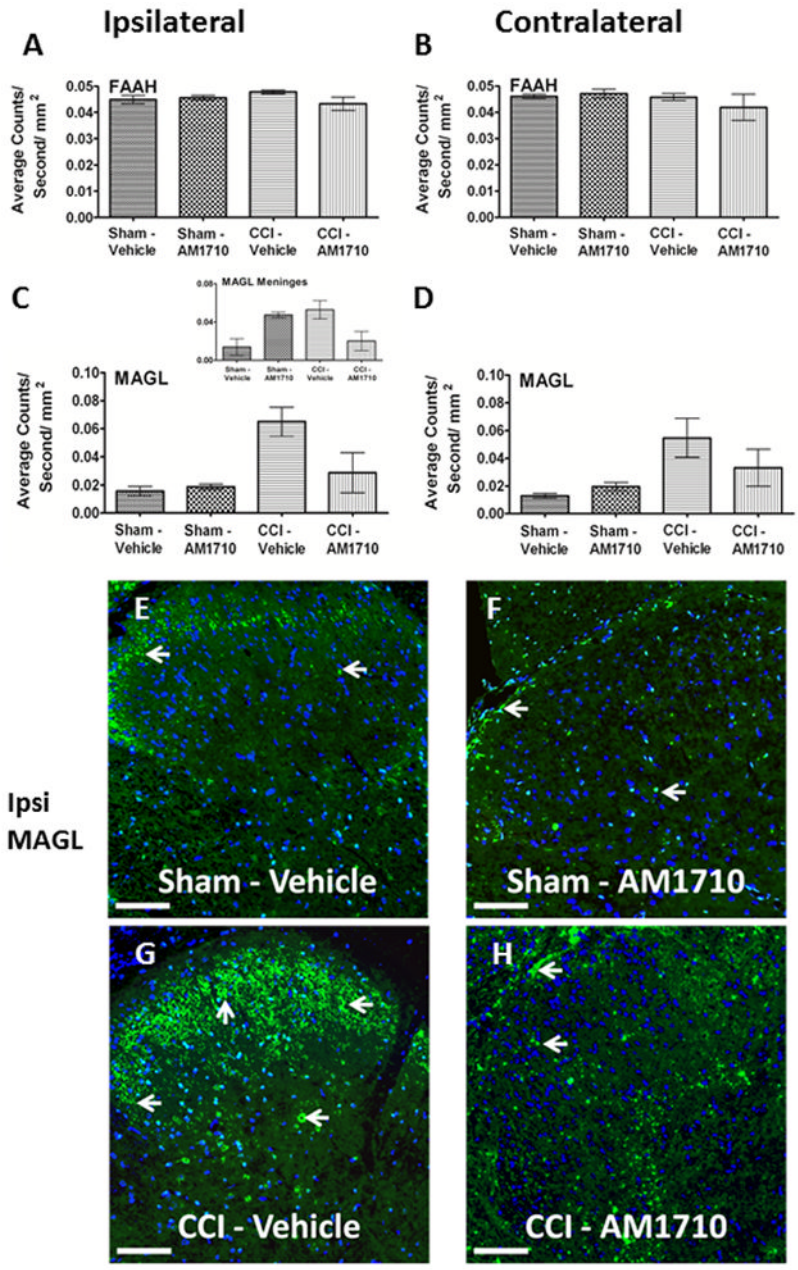

Figure 4.

Immunofluorescent intensity quantification of the spinal cord dorsal horn reveals i.t. AM1710 reduces the expression of the endocannabinoid degragative enzyme, MAGL. **A**, **B**, No changes in expression of FAAH IR between non-neuropathic sham and neuropathic CCI rats following i.t. AM1710 or equivolume vehicle were observed (ANOVA, $F_{(3,11)}$=1.967; p=0.1976; ANOVA, $F_{(3,11)}$=3.068; p=0.0910, respectively) **C**, **D**, Compared to non-neuropathic sham operated rats given i.t. AM1710 or equivolume vehicle, neuropathic rats given i.t. vehicle showed a robust bilateral increase in dorsal horn MAGL IR. In contrast, an i.t. AM1710 injection robustly suppressed bilateral increases in dorsal spinal MAGL IR (ANOVA, $F_{(3,11)}$=11.38; p=0.0029, ANOVA, $F_{(3,11)}$=5.444; p=0.00247, respectively). **Inset, C,** non-neuropathic sham rats given i.t. AM1710 as well as neuropathic rats given i.t. vehicle showed an increase in meningeal MAGL IR compared to non-neuropathic rats given

i.t. vehicle (ANOVA, $F_{(3,11)}$=8.153; p=0.0081). **E**, **F**, **G**, **H**, Representative spectrally unmixed images at 20x magnification of MAGL fluorescent staining (green), and DAPI nuclear stain (blue). In all images the scale bar is equal to 50 μm.

NIH-PA Author Manuscript
NIH-PA Author Manuscript
NIH-PA Author Manuscript

NIH-PA Author Manuscript
NIH-PA Author Manuscript
NIH-PA Author Manuscript

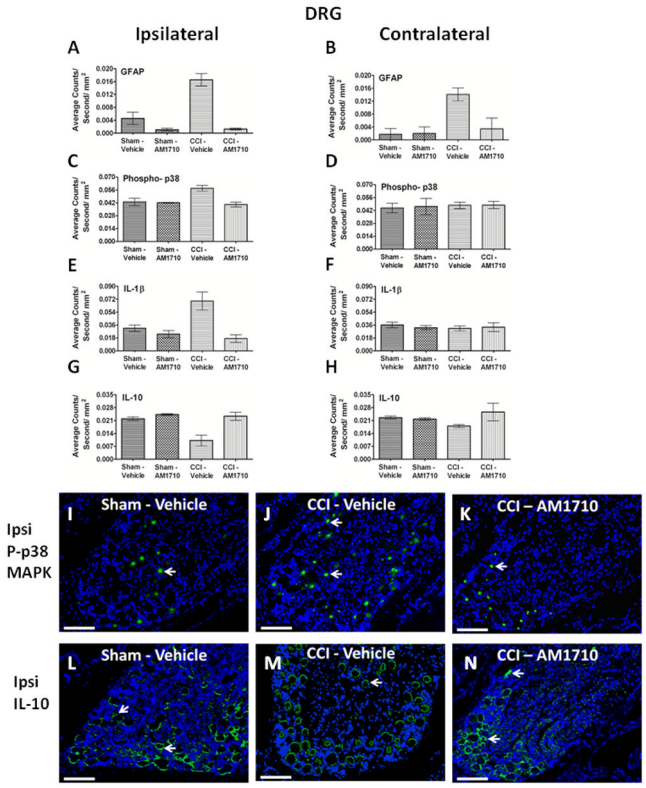

Figure 5.

Immunofluorescent intensity quantification of the dorsal root ganglion reveals differences in astrocyte activation levels, phosphorylated p38MAPK, IL1β and IL-10. **A**, **B**, Compared to non-neuropathic sham operated rats given i.t. AM1710 or equivolume vehicle, CCI-induced neuropathic rats given i.t. vehicle revealed a robust bilateral increase in GFAP IR. However, i.t. AM1710 injection robustly blocked bilateral increases in GFAP IR (ANOVA, $F_{(3,11)}$=28.56; p=0.0001, ANOVA, $F_{(3,11)}$=6.067; p=0.0186, respectively). **C**, **D**, DRG changes in levels of p-p38MAPK IR occurred in the ipsilateral(ANOVA, $F_{(3,11)}$=8.097; p=0.0083), but not the contralateral (ANOVA, $F_{(3,11)}$=0.01644; p=0.9969) spinal cord to the sciatic nerve damage. **E, F,** Unilateral change was also observed with IL-1β IR (ipsilateral ANOVA, $F_{(3,11)}$=9.291; p=0.0055, contralateral ANOVA, $F_{(3,11)}$=0.2395; p=0.8664). **G, H**, IL-10 IR was also unilaterally decreased in neuropathic animals following CCI surgery given i.t. vehicle treatment of AM1710 (ipsilateral ANOVA, $F_{(3,11)}$=12.01; p=0.0025, contralateral ANOVA, $F_{(3,11)}$=1.612; p=0.2618). **I, J, K**, Representative spectrally unmixed images of phospho-p38 at 20x magnification, phospho-p38 fluorescent staining (green) and DAPI nuclear stain (blue). **L**, **M**, **N**, IL-10 representative spectrally unmixed images at 20x, IL-10 fluorescent staining (green) and DAPI nuclear stain (blue). In all images the scale bar is equal to 50 μm.

NIH-PA Author Manuscript
NIH-PA Author Manuscript
NIH-PA Author Manuscript

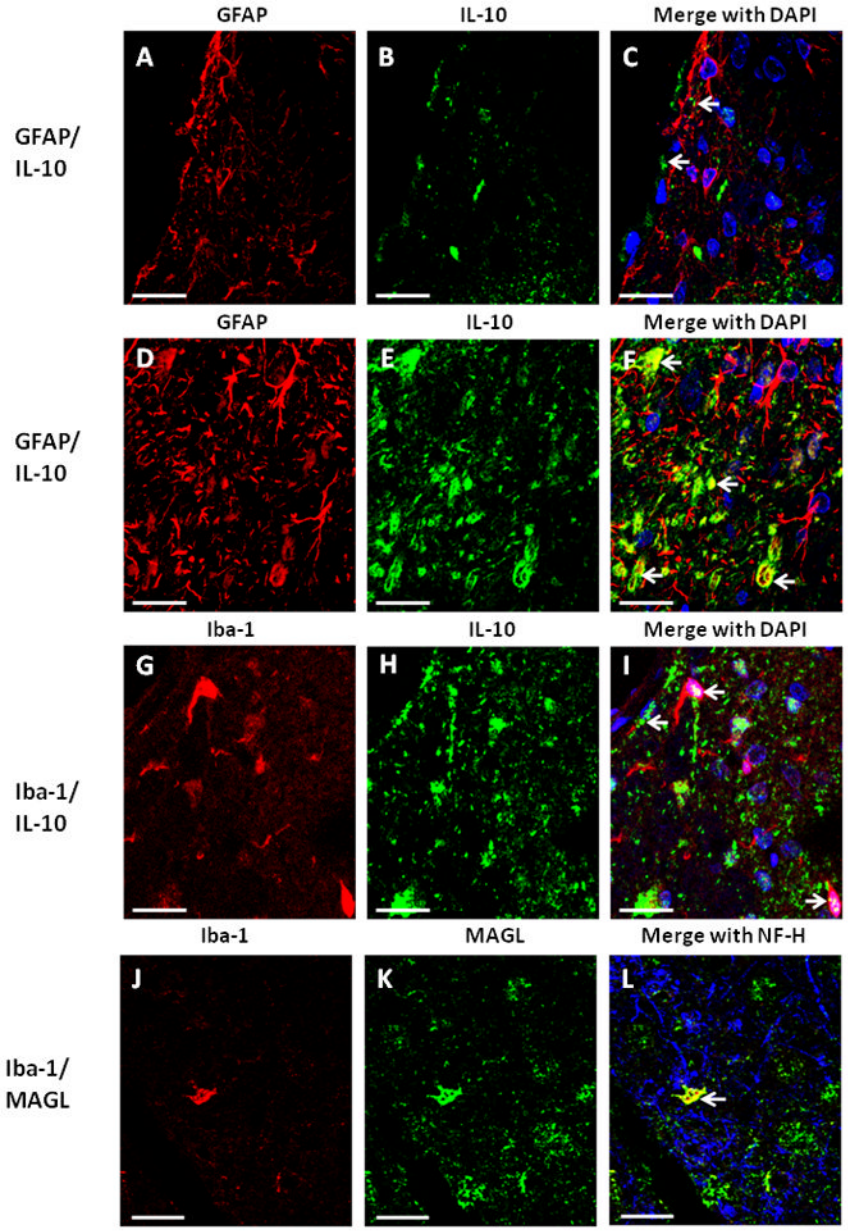

Figure 6.

Qualitative confocal images of cellular immunostaining of IL-10 in spinal cord. **A**–**I,** Spinal cord tissue from rats with CCI-AM1710 treatment. **A**, **B**, **C**, Immunostaining of IL-10 (green) in meninges and superficial laminae of the spinal cord dorsal horn is *not* co-labeled with GFAP (red) positive cells. DAPI nuclear labeling is blue. Arrows indicate IL-10 in the superficial laminae. **D**, **E**, **F,** Immunostaining of IL-10 (green) in the deeper laminae of the dorsal horn spinal cord is co-labeled yellow with GFAP (red) positive cells, with DAPI nuclear labeling (blue). Arrows indicate co-labeling of IL-10 and GFAP positive cells. **G**, **H**, **I**, Immunostaining of IL-10 (green) in the meninges and superficial laminae of the dorsal horn spinal cord is co-labeled (yellow) with Iba-1 (red) positive cells, with DAPI nuclear labeling (blue). Arrows indicate co-labeling of IL-10 and Iba-1 positive cells. **J**, **K**,**L**, Immunostaining of MAGL (green) in the deeper laminae of the dorsal horn is co-labeled yellow with Iba-1 (red) positive cells, with NF-H neuronal labeling (blue). An arrow

indicates co-labeling of MAGL and an Iba-1 positive cell. In all images the scale bar is equal to 20 μm.

NIH-PA Author Manuscript
NIH-PA Author Manuscript
NIH-PA Author Manuscript

NIH-PA Author Manuscript
NIH-PA Author Manuscript
NIH-PA Author Manuscript

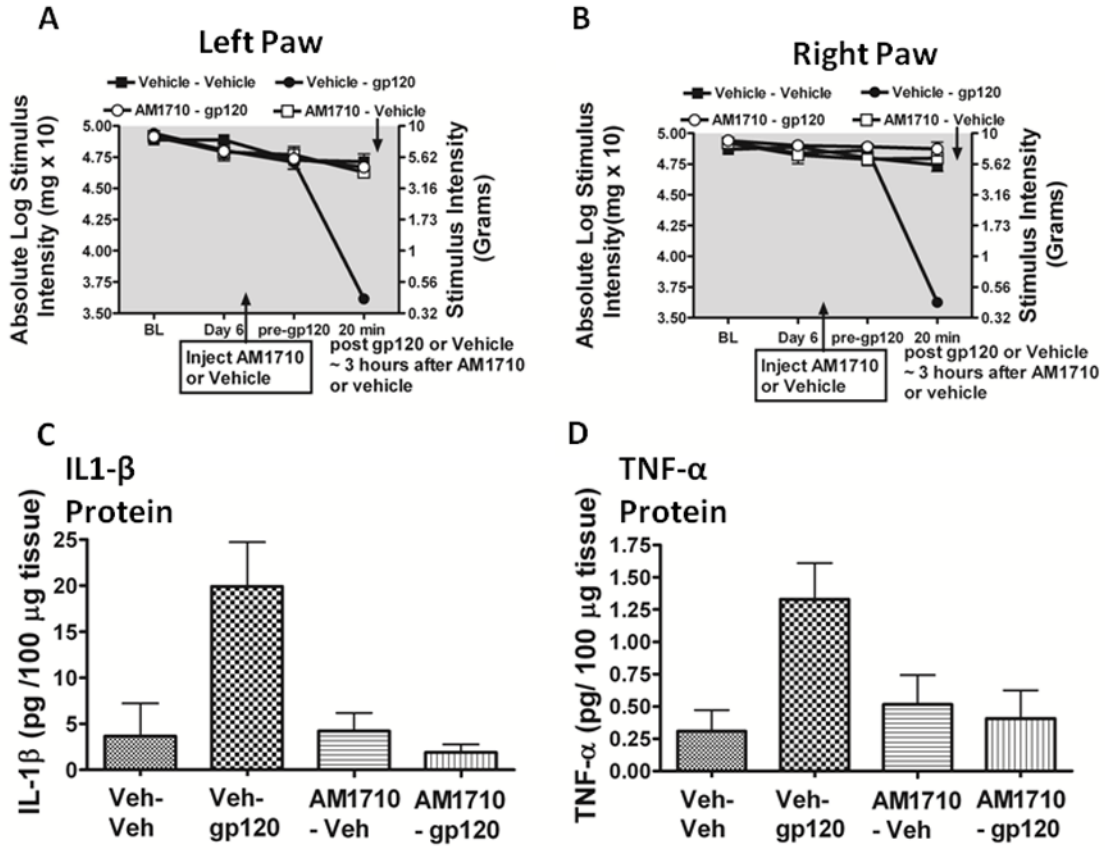

Figure 7.

AM1710 pre-treatment blocks gp120-induced allodynia and IL-1β cytokine production. A total of 24 animals were used for both the behavioral experiment reported here and tissues from these animals were analyzed in the reported ELISA experiments. **A**, **B**, Prior to surgical manipulation, all groups exhibited similar bilateral (ipsilateral and contralateral) BL thresholds (ANOVA, $F_{(3,23)}$ =1.781; p=0.1833; $F_{(3,23)}$ =2.311; p=0.1072, respectively). Following indwelling catheter implantation, there was no major effect of surgery on Day 6 after surgery thresholds when compared to BL thresholds or following the i.t. pretreatment of either AM1710 or vehicle (ANOVA, $F_{(6,60)}$ = 0.9381; p=0.1311; ANOVA, $F_{(6,60)}$=2.415 ; p=0.1648, respectively). Animals given i.t. gp120 developed strong allodynia in both left and right paws at 20 min compared to pre-gp120 threshold values (ANOVA, $F_{(3,20)}$=61.72; p<0.0001 ANOVA, $F_{(3,20)}$=75.73; p<0.0001, respectively). **C**, Quantification of IL-1β protein by ELISA revealed IL-1β was significantly increased in left DRG of allodynic rats following i.t. gp120 given a pretreatment with i.t. vehicle of AM1710 (ANOVA, $F_{(3,13)}$= 7.785; p=0.0057). **D**, a trend in the levels of TNF-α protein, although not statistically significant (ANOVA, $F_{(3,14)}$ = 2.977; p=0.0741).

NIH-PA Author Manuscript NIH-PA Author Manuscript NIH-PA Author Manuscript

Pain. Author manuscript; available in PMC 2013 May 01.

Table 1

List of all antibodies used in this study and designated under the appropriate column heading. Primary antibodies for polyclonal GFAP (astrocyte specific glial fibrillary acidic protein, Millipore, Billerica, MA, and Abcam, Cambridge, MA), monoclonal GFAP (astrocyte specific glial fibrillary acidic protein, Progen, Heidelberg, Germany), Iba-1 (microglia, monocyte specific calcium channel protein, Wako Chemicals, Osaka, Japan), FAAH (fatty acid amide hydrolase endocannabinoid degredgative enzyme, Cayman Chemicals, Ann Arbor, MI), IL-1β protein (proinflammatory cytokine, Santa Cruz Biotechnology, Santa Cruz, CA), NF-H 200KDa (neurofiliament heavy chain clone 3G3, Millipore, Billerica, MA), MAGL (monoacylglyerol lipase endocannabinoid dregradative enzyme, Abcam, Cambridge, MA), phosphorylated p38MAPK (activated proinflammatory cytokine signaling pathway, Cell Signaling Technology, Beverly, MA) and IL-10 protein (anti-inflammatory cytokine, R&D Systems, Minneapolis, MN) were used. Secondary antibody incubation was performed with the indicated fluorophore conjugated secondary antibody. For MAGL, phosphorylated p38MAPK, and IL-10 protein, after overnight primary incubation, sections were instead incubated with biotinylated secondary antibody.

Primary antibody	Antibody clone	Indication	Anatomical region	Vendor	Host	Dilution used	Antigen retrieval	TSA used	Secondary Antibody*
GFAP	Polyclonal	Astrocyte	Dorsal Horn Spinal Cord	Millipore	Rabbit	1:1000	Tris Buffer	No	Rhodamine Red Donkey anti-Rabbit (1:200)
GFAP	Polyclonal	Astrocyte	Dorsal Horn Spinal Cord	Abcam	Chicken	1:1000	Tris Buffer	No	AMCA, CY-5 Donkey anti-Chicken (1:200)
GFAP	Monoclonal	Astrocyte	DRG	Progen	Rabbit	1:10	Citrate Buffer	No	Rhodamine Red Donkey anti-Rabbit (1:200)
Iba-1	Polyclonal	Microglia	Dorsal Horn Spinal Cord	Wako	Rabbit	1:300	Tris Buffer	No	Rhodamine Red, FITC Donkey anti-Rabbit (1:200)
FAAH	Polyclonal	Ecb enzyme	Dorsal Horn Spinal Cord	Cayman Chemical	Rabbit	1:100	Tris Buffer	No	Rhodamine red Donkey anti-Rabbit (1:200)
MAGL	Polyclonal	Ecb enzyme	Dorsal Horn Spinal Cord	Abcam	Rabbit	1:100	Citrate Buffer	Yes	Biotinylated Donkey anti-Rabbit (1:1300)
p-p38	Polyclonal	Phospho-p38 MAP Kinase	Dorsal Horn Spinal Cord, DRG	Cell Signalling	Rabbit	1:800	Citrate Buffer	Yes	Biotinylated Donkey anti-Rabbit (1:1300)
IL-10	Polyclonal	IL-10 Protein	Dorsal Horn Spinal Cord, DRG	R&D Systems	Goat	1:250	Citrate Buffer	Yes	Biotinylated Donkey anti-Goat (1:1300)
IL-1β	Polyclonal	IL-1 beta Protein	Dorsal Horn Spinal Cord, DRG	Santa cruz	Rabbit	1:300	Tris Buffer	No	Rhodamine Red Donkey anti-Rabbit (1:200)
NF-H 200	Monoclonal	Neuron	Dorsal Horn Spinal Cord, DRG	Millipore	Mouse	1:100	Citrate Buffer	No	Rhodamine Red Donkey anti-Mouse (1:200)

*All secondary antibodies are from Jackson Immunoresearch (West Grove, PA).